P_c IN THE PENTAQUARK PICTURE

Wiriya Ruangyoo

A Thesis Submitted in Partial Fulfillment of the Requirements for the

Degree of Master of Science in Physics

Suranaree University of Technology

Academic Year 2020

P_c ในรูปแบบการจำลองแบบเพนตะควาร์ก

นายวิริยะ เรืองอยู่

วิทยานิพนธ์นี้เป็นส่วนหนึ่งของการศึกษาตามหลักสูตรปริญญาวิทยาศาสตรมหาบัณฑิต
สาขาวิชาฟิสิกส์
มหาวิทยาลัยเทคโนโลยีสุรนารี
ปีการศึกษา 2563

P_c IN THE PENTAQUARK PICTURE

Suranaree University of Technology has approved this thesis submitted in partial fulfillment of the requirements for a Master degree.

Thesis Examining Committee

(Assoc. Prof. Dr. Yi Yang)
Chairperson

(Asst. Prof. Dr. Ayut Limphirat)
Member (Advisor)

(Prof. Dr. Yupeng Yan)
Member (Co-Advisor)

(Prof. Dr. Chia-Chu Chen)
Member (Co-Advisor)

(Asst. Prof. Dr. Christoph Herold)
Member

(Assoc.Prof.Flt.Lt.Dr.Kontorn Chamniprasart)
Vice Rector for Academic Affairs
and Internationalization

(Assoc.Prof.Dr.Worawat Meevasana)
Dean of Institute of Science

วีริยะ เรืองอยู่ : P_c ในรูปแบบการจำลองแบบเพนตะควาร์ก (P_c IN THE PENTAQUARK PICTURE) อาจารย์ที่ปรึกษาวิทยานิพนธ์ : ผู้ช่วยศาสตราจารย์ ดร.อายุทธ ลิ้มพิรัตน์, 68 หน้า

จากการตรวจพบเพนตะควาร์กโดย LHCb นักฟิสิกส์จึงพยายามที่จะอธิบายโครงสร้างภายในและความเป็นไปได้ของกระบวนการสลายตัว รวมไปถึงเลขควอนตัมที่เป็นไปได้ของเพนตะควาร์ก ซึ่งในงานวิจัยนี้ได้สร้างฟังก์ชันคลื่นของเพนตะควาร์กโดยใช้แบบจำลองควาร์กภายใต้สมมุติฐานว่า เพนตะควาร์กที่ตรวจพบเป็นอนุภาคเพนตะควาร์กแท้ โดยสร้างจากฟังก์ชันคลื่นที่ประกอบด้วย 3 ควาร์กเบา และคู่ควาร์ก-ปฏิควาร์กหนัก จากเงื่อนไขฟังก์ชันคลื่นของสีในแต่ละอนุภาคจะต้องมีการจัดเรียงแบบซิงเกลต (Color singlet) ซึ่งพบว่าเพนตะควาร์กมีจัดเรียงของสีสองความเป็นไปได้ คือ ซิงเกลต-ซิงเกลต ($[111]_{qqq}\otimes[111]_{c\bar{c}}$) และออกเตต-ออกเตต ($[21]_{qqq}\otimes[21]_{c\bar{c}}$) ทั้งนี้จะได้ฟังก์ชันคลื่นของเพนตะควาร์กที่เป็นไปได้ทั้งหมดจำนวน 17 สถานะ ที่นำไปคำนวณหาแอมพลิจูดการเปลี่ยนผ่านและอัตราส่วนความกว้างการสลายของอนุภาคระหว่างเพนตะควาร์กและสถานะการสลายตัวของอนุภาคสุดท้ายที่เป็นไปได้ จากการคำนวณพบว่าช่องทางการสลายตัวของ pJ/ψ มีค่าความกว้างการสลายตัวมากกว่าช่องทางการสลายตัวอื่นๆ อีกทั้งอัตราส่วนความกว้างการสลายตัว แสดงให้เห็นว่า หากสถานะของเพนตะควาร์กไม่มีการผสมสถานะในเลขควอนตัมเดียวกัน ทั้งสถานะ $I=\frac{1}{2}$ และ $J=\frac{3}{2}$ และสถานะ $I=\frac{1}{2}$ และ $J=\frac{1}{2}$ จะมีค่าการสลายตัวของอนุภาคที่เกิดในช่องทางของ pJ/ψ เท่ากัน ซึ่งบ่งชี้ได้ว่า $P_c(4440)$ อาจไม่ใช่โครงสร้างแบบเพนตะควาร์กแท้ เนื่องจากความกว้างของการสลายตัวที่วัดได้จากการทดลองมีค่าสูงกว่าเพนตะ-ควาร์กอื่น ๆ มาก อีกทั้งยังบ่งชี้ให้เห็นอีกว่า $P_c(4312)$ มีความเป็นไปได้ที่จะมีค่าของสปินเท่ากับ $\frac{1}{2}$ ในขณะที่สปินเท่ากับ $\frac{3}{2}$ อาจเป็นไปได้ที่จะกำหนดให้เป็น $P_c(4457)$ ตามคำแนะนำของ LHCb วิทยานิพนธ์นี้ยังได้การสร้างสถานะของเพนตะควาร์กที่เป็นไปได้ทั้งหมดโดยใช้ทฤษฎีกลุ่มและสถานะของเพนตะควาร์กในช่องทางการสลายตัวอื่น ๆ ซึ่งผลการทดลองนี้จะได้รับการตรวจพบและยืนยันด้วยผลการทดลองในอนาคต

สาขาวิชาฟิสิกส์ ลายมือชื่อนักศึกษา วีริยะ เรืองอยู่

ปีการศึกษา 2563 ลายมือชื่ออาจารย์ที่ปรึกษา

ลายมือชื่อที่ปรึกษาร่วม Yupeng Yan

ลายมือชื่อที่ปรึกษาร่วม Chia Chu Chen

WIRIYA RUANGYOO : P_c IN THE PENTAQUARK PICTURE

ADVISOR : ASST. PROF. AYUT LIMPHIRAT, Ph.D. 68 PP.

PENTAQUARK/ QUARK MODEL/ PARTIAL WIDTH RATIO

Since the pentaquark discovery in the LHCb collaboration, physicists have tried to describe its structure and possible decay processes, resulting in the determination of the quantum numbers of the pentaquark. In this research, we constructed the pentaquark wave functions by using the quark model under the compact pentaquark picture. The wave function was derived from the combination of 3 light quarks and heavy quark-antiquark pair ($c\bar{c}$). There are two possible color singlets for pentaquarks, which are the combination of color singlet-singlet ($[111]_{qqq} \otimes [111]_{c\bar{c}}$) and color octet-octet ($[21]_{qqq} \otimes [21]_{c\bar{c}}$). The possible pentaquark configurations can be in 17 states. The transition amplitudes and partial width ratios were calculated between the pentaquark states and the possible decay channel states. We found that the decay channels pJ/ψ remained dominant when compared with other decay channels. Meanwhile, the partial width ratio showed that if there is no mixing among the $I = \frac{1}{2}$ and $J = \frac{3}{2}$ states as well as among the $I = \frac{1}{2}$ and $J = \frac{1}{2}$ states, the two states in pJ/ψ channel have the same decay widths, which indicates that $P_c(4440)$ may not be a compact pentaquark state since its decay width is much larger than others. Our results suggested that $P_c(4312)$ might be a spin-$\frac{1}{2}$ particle while the spin-$\frac{3}{2}$ may be assigned to $P_c(4457)$. Moreover, this work constructs all possible pentaquark states by using group theory, and the pentaquark states in other decay channels discussed in this thesis can be possibly searched and confirmed in the future.

School of Physics

Academic Year 2020

Student's Signature ____________________

Advisor's Signature ____________________

Co-advisor's Signature ____________________

Co-advisor's Signature ____________________

ACKNOWLEDGEMENTS

Firstly, I am very grateful to Asst. Prof. Dr. Ayut Limphirat, Prof. Dr. Yupeng Yan, and Prof. Dr. Chia-Chu Chen for being my thesis advisor and co-advisors. The professors have pushed me toward a new experience and suggested me to enroll in the dual/double degree program at National Cheng Kung University, Taiwan. They have taught me valuable lessons and have guided me through tough theoretical physic concepts. More specifically, they provided massive assistance during result analysis. Without their help, this thesis would not possible to accomplish.

I would like to thank Asst. Prof. Dr. Christoph Herold and Assoc. Prof. Dr. Yi Yang for sitting as the thesis committee as well as for offering excellent advice.

I would like to thank the School of Physics, Suranaree University of Technology and the Department of Physics, National Cheng Kung University for allowing me to study their dual/double degree program in physics. I express my deep gratitude to both parties for their support throughout my studies. Moreover, I thank the Development and Promotion of Science and Technology Talents (DPST) Project for their scholarship.

I would like to thank all physics lecturers of both universities, who have taught me and made it possible for the expansion of my knowledge in the past three academic years. Many thanks to my friends and seniors, especially Mr. Kai Xu and Mr. Attaphon Kaewsanod, for those valuable discussions and suggestions.

I would like to thank all the staff who have helped me with the application process and processing the necessary documents in both universities.

Last but not least, I also would like to thank my family and my friends for their support and encouragement. Without their support, my thesis would not be accomplished. I am truly grateful for their love, support, and close attention during hardship.

Wiriya Ruangyoo

CONTENTS

CONTENTS (Continued)

LIST OF FIGURES

LIST OF TABLES

LIST OF TABLES (Continued)

CHAPTER I

INTRODUCTION

Various types of particles were discovered in hadron colliders over the past centuries. In 1964, the quark model was proposed by Gell-Mann and Zweig to study the inner structure of hadrons (Gell-Mann, 1964; Zweig, 1964) to classify the then observed particles. The basic picture of the quark model is that baryons and mesons are composed of three quarks (qqq) and quark-antiquark ($q\bar{q}$), respectively.

In recent years, various efficient theoretical approaches have been developed to investigate hadronic structure such as chiral quark-soliton model (Liu et al., 2019), and the nonperturbative effect of Quantum Chromodynamics (QCD), including phenomenological model such as QCD inspired model. Amongst various approaches, the quark model is still a successful method in understanding and describing the characteristics and properties of hadronic systems. For instance, the mass of the Ω^- was predicted by Gell-Mann and experimentally detected in 1964 by Barnes and others (Barnes et al., 1964). Many years later, the quark model was still employed to study hadronic structure such as the nucleon and its lower-lying resonances (Yan et al., 2003; Yan et al., 2010) as well as the states of the Ξ_b (Limphirat et al., 2010).

Quark model concepts are also applied to explain the exotic hadrons which include more quark contents than the ordinary baryon and meson. It is interesting to study the multiquark system, such as exotic mesons named tetraquark (2-quarks and 2-antiquarks bound state) and pentaquark or exotic baryons (4-quark and 1-antiquark bound state). Since 2003, many observations have reported these possible exotic hadrons. The first observation of Θ^+ pentaquark was reported by LEPS (Yao et al., 2006) but there has not been enough information to justify that it is a pentaquark state. In 2015, the $\Lambda_b^0 \to pJ/\psi K^-$ decay process was studied by the LHCb collaboration (Aaij et al., 2015). They proposed two possible decay processes, one is the process $\Lambda_b^0 \to \Lambda^* J/\psi$ with $\Lambda^* \to pK^-$. The experimental data were fitted by using the 14 Λ^* states with the invariant mass of K^-p. The results of this fitting were not a satisfactory explanation for the $\Lambda^* \to pK^-$ channel. The other process is the $\Lambda_b^0 \to P_c^+ K^-$ where P_c^+ is the hidden-charm pentaquark states which were observed in the pJ/ψ channels ($P_c^+ \to pJ/\psi$) at 7 and 8 TeV proton-proton collisions. There are two pentaquarks which were reported on this observation, the $P_c(4380)$ and the $P_c(4450)$. $P_c(4380)$ has a mass spectrum of $4380 \pm 8 \pm 29$ MeV and a width of $205 \pm 18 \pm 86$ MeV. The $P_c(4450)$ has a mass spectrum of $4449.8 \pm 1.7 \pm 2.5$ MeV and a width of $39 \pm 5 \pm 19$ MeV. The analysis of the angular distribution of two P_c leads to the possible quantum number J^P as $\frac{3}{2}^-$ and $\frac{5}{2}^+$ despite a possible combination between the two. Moreover, the acceptable quantum numbers in the cases with opposite parity is also found as either $(\frac{3}{2}^+, \frac{5}{2}^-)$ or $(\frac{5}{2}^+, \frac{3}{2}^-)$.

In 2019, LHCb collaboration combined the data between Run 1 (pp collision energies of 7 and 8 TeV) and Run 2 (pp collision energy of 13 TeV). The new resonance $P_c(4312)$ was observed, whose mass is $4311.9 \pm 0.7^{+6.8}_{-0.6}$ MeV with a width of $9.8 \pm 2.7^{+3.7}_{-4.5}$ MeV. The $P_c(4450)$ pentaquark structure in the previous report is resulted as the overlapped between two peaks which are the $P_c(4440)$ and the $P_c(4457)$. Both narrow peaks have respective masses of $4440.3 \pm 1.3^{-4.1}_{-4.7}$ MeV and $4457.3 \pm 0.6^{-4.1}_{-4.7}$ MeV and widths of $20.6 \pm 4.9^{+8.7}_{-10.1}$ MeV and $6.4 \pm 2.0^{+5.7}_{-1.9}$ MeV. The spin and parity of these P_c states have not been reported, they are only suggested the possible quantum numbers as $\frac{1}{2}^-$, $\frac{1}{2}^-$, and $\frac{3}{2}^-$ for the $P_c(4312)$, $P_c(4440)$ and $P_c(4457)$, respectively. Moreover, the LHCb suggested that the P_c states are the bound state between a baryon and a meson due to the masses of the $P_c(4312)$ and the $P_c(4457)$ states are approximately 5 MeV and 2 MeV below the $\Sigma_c^+ \bar{D}^0$ and the $\Sigma_c^+ \bar{D}^{*0}$ at thresholds, respectively. While the $P_c(4440)^+$ can be $\Sigma_c^+ \bar{D}^*$ below about 20 MeV. For a broad P_c peak, the data can neither confirm nor exclude existence of the $P_c(4380)$ state (Aaij et al., 2019). The $P_c(4380)$ state may be overlapping peaks like $P_c(4450)$. Due to insufficient information, we did not include the $P_c(4380)$ in this thesis.

At the same time, the J/ψ resonances in the $\Lambda_b^0 \to pJ/\psi K^-$ process was repeated by ATLAS collaboration and D0 collaboration (ATLAS, 2019; Abazov et al., 2019). Both collaborations confirmed the mass spectra and widths of $P_c(4440)$ and $P_c(4457)$ which are consistent with LHCb experiment except the $P_c(4312)$ pentaquark.

In 2020, the decay process $\Lambda_b^0 \to p\eta_c K^-$ was reported by LHCb for the first time. The branching fraction of decay was measured by using $\Lambda_b^0 \to pJ/\psi K^-$ as a normalisation mode, which is $BR(\Lambda_b^0 \to p\eta_c K^-) = (1.06 \pm 0.16 \pm 0.06^{+0.22}_{-0.19}) \times 10^{-4}$. The mass spectrum of $p\eta_c$ is not evidently the $P_c(4312)^+$ pentaquark state (Aaij et al., 2020), which is predicted theoretically.

Although the evidence of the P_c peak structures was suggested with the molecular picture because of the masses close to the $\Sigma_c^+ \bar{D}^{(*)0}$ at threshold and observed only in the pJ/ψ decay channel, the nature of P_c is still an open question about its structure and possible decay modes. In this work, we study the P_c^+ in the compact pentaquark picture. We work out all possible configurations with possible decay channels in the quark content of $uud c\bar{c}$.

CHAPTER II

HADRON WAVE FUNCTIONS IN QUARK MODEL

To study the P_c decay channels, one needs to construct the wave functions of the initial and final states. We suppose that the initial particle is a P_c compact pentaquark in this thesis, and the final particles are baryon and meson. In this chapter, we constructed the wave functions of hadrons in the quark model. The wave function was derived from four degrees of freedom, which are spin, flavor, color, and spatial. The configurations of spin, flavor, and color were studied and worked out by group theory. The general form of the total wave function can be represented as

$$\Psi = \psi_{spatial}\psi_{spin}\psi_{flavor}\psi_{color}. \tag{2.1}$$

Ψ has to be a totally antisymmetric wave function. Due to quark confinement, the color of hadrons should be color singlet for any multiquark systems.

2.1 The P_c Wave Functions

We assume the quark contents inside the P_c structure as $uudc\bar{c}$. The internal degree of freedom in terms of flavor is u, d, and s of $SU(3)$ symmetry, excluding charmed quark (c) and anticharm quark ($\bar{c}$). All quarks are spin-$\frac{1}{2}$ particles with colors of R, G, and B of $SU(3)$. Antiquarks transform under the conjugate fundamental representation. The construction of P_c wave function was considered in terms of a combination of q^3 and quark-antiquark pair ($c\bar{c}$) in this thesis. The q^3 and quark-antiquark pair ($c\bar{c}$) are combined to form the compact pentaquark according to color confinement of hadrons, which dictates the color wave function must be a color singlet. Thus, the wave function $\psi^C_{[222]}$ is required for pentaquark, which is represented as

$$\psi^C_{[222]} = \ydiagram{2,2,2} \quad . \tag{2.2}$$

In the language of group theory, we can represent the permutation group by Young tabloids (see Appendix A). We have two possible combinations of Young tabloid from the direct product of the color wave functions of the q^3 and quark-antiquark pair ($c\bar{c}$) to get the color singlet of pentaquark ($[222]_C$). It can either be the color singlet-singlet or component of color octet-octet, which are

1. $\psi^C_{[111]}(q^3) \otimes \psi^C_{[111]}(c\bar{c})$:

$$\psi^C_{[111]}(q^3) \otimes \psi^C_{[111]}(c\bar{c}) = \ydiagram{1,1,1} \otimes \ydiagram{1,1,1} \tag{2.3}$$

2. $\psi^C_{[21]}(q^3) \otimes \psi^C_{[21]}(c\bar{c})$:

$$\psi^C_{[21]}(q^3) \otimes \psi^C_{[21]}(c\bar{c}) = \ydiagram{2,1} \otimes \ydiagram{2,1} \tag{2.4}$$

2.1.1 Wave Functions of q^3

In the part of q^3, we demonstrate the combination of the total wave function which depends on the possible construction of color singlet. The total wave function can be described in the general form with the color wave functions (ψ^C) and orbital-spin-flavor wave functions (ψ^{OSF}) in different permutation symmetries, and takes the form as

$$\Psi_{Asym} = \sum_{i=S,A,\rho,\lambda} \sum_{j=S,A,\rho,\lambda} a_{ij} \psi^C_i \psi^{OSF}_j \tag{2.5}$$

where S, A, ρ and λ are symmetric, antisymmetric, mixed-symmetric, and mixed-antisymmetric, respectively. The four types are representations of S_3 permutation group.

They can be written in the permutation as $[3]$, $[111]$, $[21]_\rho$, and $[21]_\lambda$, respectively.

From the possible color singlet of the pentaquark, we can determine the total wave function of the particle. There are two possible forms of the q^3 part which follows from Eq. (2.5).

(a) For color singlet ($[111]_C$),

$$\Psi_{[111]}(q^3) = \psi^C_{[111]}\psi^{OSF}_{[3]}, \tag{2.6}$$

where $\Psi^C_{[111]}$ is totally antisymmetric and $\psi^{OSF}_{[3]}$ is totally symmetric.

(b) For color octet ($[21]_C$),

$$\Psi_{[21]}(q^3) = \sum_{i=\rho,\lambda}\sum_{j=\rho,\lambda} a_{ij}\psi^C_{[21]_i}\psi^{OSF}_{[21]_j}, \tag{2.7}$$

where $\psi^C_{[21]} \otimes \psi^{OSF}_{[21]}$ provides a singlet as indicated in Eq. (2.4).

Applying (12) element of the S_3 group of permutation in Appendix A, we obtain the wave function of color octet (Eq. 2.7) as

$$\begin{aligned}(12)\Psi_{[21]}(q^3) &= -\Psi_{[21]}(q^3)\\ &= a_{\lambda,\lambda}\psi^C_{[21]_\lambda}\psi^{OSF}_{[21]_\lambda} - a_{\lambda,\rho}\psi^C_{[21]_\lambda}\psi^{OSF}_{[21]_\rho} - a_{\rho,\lambda}\psi^C_{[21]_\rho}\psi^{OSF}_{[21]_\lambda} + a_{\rho,\rho}\psi^C_{[21]_\rho}\psi^{OSF}_{[21]_\rho},\end{aligned} \tag{2.8}$$

if $\Psi_{[21]}(q^3)$ is the fully antisymmetric wave function, $\Psi[21](q^3) + (12)\Psi[21](q^3)$ must be zero.

$$\Psi[21](q^3) + (12)\Psi[21](q^3) = 0 = a_{\lambda,\lambda}\psi^C_{[21]_\lambda}\psi^{OSF}_{[21]_\lambda} + a_{\rho,\rho}\psi^C_{[21]_\rho}\psi^{OSF}_{[21]_\rho}, \tag{2.9}$$

hence $a_{\lambda,\lambda} = a_{\rho,\rho} = 0$, we get

$$\Psi_{[21]}(q^3) = a_{\lambda,\rho}\psi^C_{[21]_\lambda}\psi^{OSF}_{[21]_\rho} + a_{\rho,\lambda}\psi^C_{[21]_\rho}\psi^{OSF}_{[21]_\lambda}. \tag{2.10}$$

By applying (23) element of the S_3 group of permutation, we get

$$\begin{aligned}(23)\Psi_{[21]}(q^3) &= -\Psi_{[21]}(q^3)\\ &= a_{\lambda,\rho}(-\frac{1}{2}\psi^C_{[21]_\lambda} + \frac{\sqrt{3}}{2}\psi^C_{[21]_\rho})(-\frac{1}{2}\psi^{OSF}_{[21]_\lambda} + \frac{\sqrt{3}}{2}\psi^{OSF}_{[21]_\rho}) \\ &+ a_{\rho,\lambda}(\frac{\sqrt{3}}{2}\psi^C_{[21]_\rho} + \frac{1}{2}\psi^C_{[21]_\lambda})(\frac{\sqrt{3}}{2}\psi^{OSF}_{[21]_\rho} + \frac{1}{2}\psi^{OSF}_{[21]_\lambda}),\end{aligned} \tag{2.11}$$

and follow the discussion in Eqs. (2.8) - (2.10), we have $a_{\lambda,\rho} = -a_{\rho,\lambda}$. The wave function takes the form,

$$\Psi_{[21]}(q^3) = \frac{1}{\sqrt{2}}(\psi^C_{[21]_\lambda}\psi^{OSF}_{[21]_\rho} - \psi^C_{[21]_\rho}\psi^{OSF}_{[21]_\lambda}). \tag{2.12}$$

Eq. (2.12) shows the total wave function for color $[21]_C$ of the q^3 part wave function.

For the spatial-spin-flavor (ψ^{OSF}) and spin-flavor (ψ^{SF}) in Eq. (2.6) and (2.12), we can find the combination of ψ^{OSF} in term ψ^O and ψ^{SF}. The ψ^{SF} can be derived in terms of ϕ and χ which are the flavor and spin wave function. We can write the general form as

$$\Psi^{OSF}_{[\lambda]} = \sum_{i=S,A,\rho,\lambda}\sum_{j=S,A,\rho,\lambda} b_{ij}\psi^O_i\psi^{SF}_j, \tag{2.13}$$

$$\Psi^{SF}_{[\lambda]} = \sum_{i=S,A,\rho,\lambda}\sum_{j=S,A,\rho,\lambda} c_{ij}\chi_i\phi_j, \tag{2.14}$$

where $[\lambda]$ is the irreducible representation of permutation group.

From Eqs. (2.6) and (2.12), we have worked out the possible configuration of ψ^{OSF} by applying S_3 permutation. The results of the combination of the spatial-spin-flavor wave function for color singlet and octet configurations are shown in Table 2.1 and Table 2.2, respectively. The results of the spin-flavor wave function are shown in Table 2.3.

Table 2.1 The spatial-spin-flavor wave function of q^3 cluster for color singlet state.

$[3]_{OSF}$	
Orbital	Spin-Flavor
$[3]_O$	$[3]_{SF}$
$[21]_O$	$[21]_{SF}$
$[111]_O$	$[111]_{SF}$

Table 2.2 the spatial-spin-flavor wave function of q^3 cluster for color octet state.

$[21]_{OSF}$	
Orbital	Spin-Flavor
$[3]_O$	$[21]_{SF}$
$[21]_O$	$[3]_{SF}$, $[21]_{SF}$, $[111]_{SF}$
$[111]_O$	$[21]_{SF}$

Table 2.3 The configuration of spin-flavor wave function for q^3 cluster.

$[3]_{FS}$	$[3]_F \otimes [3]_S$	$[21]_F \otimes [21]_S$
$[21]_{FS}$	$[3]_F \otimes [21]_S$	$[21]_F \otimes [3]_S$
	$[21]_F \otimes [21]_S$	$[111]_F \otimes [21]_S$
$[111]_{FS}$	$[21]_F \otimes [21]_S$	$[111]_F \otimes [3]_S$

The detailed wave function of q^3 part in P_c for both color singlet and octet configurations in Tables 2.1, 2.2, and 2.3 are listed in Table 2.4. We assume the q^3 wave function in the ground state.

Table 2.4 The q^3 part configuration of P_c wave function.

Color singlet model	$\psi^{O}_{[3]}\psi^{C}_{[111]}\phi_{[3]}\chi_{[3]}$
	$\psi^{O}_{[3]}\psi^{C}_{[111]}\phi_{[21]}\chi_{[21]}$
Color octet model	$\psi^{O}_{[3]}\psi^{C}_{[21]}\phi_{[3]}\chi_{[21]}$
	$\psi^{O}_{[3]}\psi^{C}_{[21]}\phi_{[21]}\chi_{[3]}$
	$\psi^{O}_{[3]}\psi^{C}_{[21]}\phi_{[21]}\chi_{[21]}$
	$\psi^{O}_{[3]}\psi^{C}_{[21]}\phi_{[21]}\chi_{[21]}$

In Table 2.3, the symmetry properties of spin-flavor wave function can be expanded to the detail in terms of combination between $SU(3)$ and $SU(2)$. The detailed wave functions are classified according to permutation symmetries in Table 2.5.

Table 2.5 Spin- flavor wave function of q^3 classified in language of permutation symmetry.

Symmetric, [3]	([3],[3]):	$\phi^{[3]}\chi^{[3]}$
	([21],[21]):	$\frac{1}{\sqrt{2}}(\phi^{[21]_\rho}\chi^{[21]_\rho} + \phi^{[21]_\lambda}\chi^{[21]_\lambda)}$
Antisymmetric, [111]	([111],[3]):	$\phi^{[111]}\chi^{[3]}$
	([21],[21]):	$\frac{1}{\sqrt{2}}(\phi^{[21]_\rho}\chi^{[21]_\rho} - \phi^{[21]_\lambda}\chi^{[21]_\lambda)}$
ρ-type, $[21]_\rho$	([3],[21]):	$\phi^{[3]}\chi^{[21]_\rho}$
	([21],[3]):	$\phi^{[21]_\rho}\chi^{[3]}$
	([21],[21]):	$\frac{1}{\sqrt{2}}(\phi^{[21]_\lambda}\chi^{[21]_\rho} + \phi^{[21]_\rho}\chi^{[21]_\lambda)}$
	([111],[21]):	$-\phi^{[111]}\chi^{[21]_\lambda}$
λ-type, $[21]_\lambda$	([3],[21]):	$\phi^{[21]}\chi^{[21]_\lambda}$
	([21],[3]):	$\phi^{[21]_\lambda}\chi^{[3]}$
	([21],[21]):	$\frac{1}{\sqrt{2}}(\phi^{[21]_\rho}\chi^{[21_\rho} - \phi^{[21]_\lambda}\chi^{[21]_\lambda)}$
	([111],[21]):	$\phi^{[111]}\chi^{[21]_\rho}$

By the way, we have worked out the spin, flavor, and color wave function by using the projection operators of S_3 in Appendix B. The explicit forms of flavor wave function are shown in Table 2.6. In the same way, the spin wave functions with the [3], $[21]_\lambda$ and $[21]_\rho$ symmetries can be derived by the projection operators. All configurations of spin for S_3 are shown in Table 2.7. We define I, I_3, S, and S_3 as the total isospin, the projection isospin, the total spin, and the projection spin, respectively. The color configuration is given in Table 2.8.

Table 2.6 Flavor wave function of q^3.

Types	Flavor (ϕ_{I,I_3})
Symmetric (ϕ_S)	$\phi_{\frac{3}{2},\frac{3}{2}} = uuu$
	$\phi_{\frac{3}{2},\frac{1}{2}} = \frac{1}{\sqrt{3}}(uud + duu + duu)$
	$\phi_{\frac{3}{2},-\frac{1}{2}} = \frac{1}{\sqrt{3}}(ddu + udd + dud)$
	$\phi_{\frac{3}{2},-\frac{3}{2}} = ddd$
λ-type (ϕ_λ)	$\phi_{\frac{1}{2},\frac{1}{2}} = \frac{1}{\sqrt{6}}(2uud - duu - udu)$
	$\phi_{\frac{1}{2},-\frac{1}{2}} = \frac{1}{\sqrt{6}}(dud + udd - 2ddu)$
ρ-type (ϕ_ρ)	$\phi_{\frac{1}{2},\frac{1}{2}} = \frac{1}{\sqrt{2}}(udu - duu)$
	$\phi_{\frac{1}{2},-\frac{1}{2}} = \frac{1}{\sqrt{2}}(udd - dud)$

Table 2.7 Spin wave function of q^3.

Types	Spin (χ_{S,S_3})
Symmetric (χ_S)	$\chi_{\frac{3}{2},\frac{3}{2}} = \lvert\uparrow\uparrow\uparrow\rangle$ $\chi_{\frac{3}{2},\frac{1}{2}} = \frac{1}{\sqrt{3}}\lvert\uparrow\uparrow\downarrow + \downarrow\uparrow\uparrow + \uparrow\downarrow\uparrow\rangle$ $\chi_{\frac{3}{2},-\frac{1}{2}} = \frac{1}{\sqrt{3}}\lvert\downarrow\downarrow\uparrow + \uparrow\downarrow\downarrow + \downarrow\uparrow\downarrow\rangle$ $\chi_{\frac{3}{2},-\frac{3}{2}} = \lvert\downarrow\downarrow\downarrow\rangle$
λ-type (χ_λ)	$\chi_{\frac{1}{2},\frac{1}{2}} = \frac{1}{\sqrt{6}}\lvert 2\uparrow\uparrow\downarrow - \downarrow\uparrow\uparrow - \uparrow\downarrow\uparrow\rangle$ $\chi_{\frac{1}{2},-\frac{1}{2}} = \frac{1}{\sqrt{6}}\lvert\downarrow\uparrow\downarrow + \uparrow\downarrow\downarrow - 2\downarrow\downarrow\uparrow\rangle$
ρ-type (χ_ρ)	$\chi_{\frac{1}{2},\frac{1}{2}} = \frac{1}{\sqrt{2}}\lvert\uparrow\downarrow\uparrow - \downarrow\uparrow\uparrow\rangle$ $\chi_{\frac{1}{2},-\frac{1}{2}} = \frac{1}{\sqrt{2}}\lvert\uparrow\downarrow\downarrow - \downarrow\uparrow\downarrow\rangle$

Table 2.8 Color wave function of q^3 part for pentaquark.

Singlet	$\frac{1}{\sqrt{6}}(RGB - RBG + GBR - GRB + BRG - BGR)$	
	ρ type	λ type
Octet		
1	$\frac{1}{\sqrt{2}}(RGR - GRR)$	$\frac{1}{\sqrt{6}}(RRG - RGR - GRR)$
2	$\frac{1}{\sqrt{2}}(RGG - GRG)$	$\frac{1}{\sqrt{6}}(RGG - GRG - 2GGR)$
3	$\frac{1}{\sqrt{2}}(RBR - BRR)$	$\frac{1}{\sqrt{6}}(2RRB - RBR - BRR)$
4	$\frac{1}{2}(RBG + GBR - BRG$ $-BGR)$	$\frac{1}{\sqrt{12}}(2RGB + 2GRB - GBR$ $-RBG - BRG - BGR)$
5	$\frac{1}{\sqrt{2}}(GBG - BGG)$	$\frac{1}{\sqrt{6}}(2GGB - GBG - BGG)$
6	$\frac{1}{\sqrt{12}}(2RGB - 2GRB - GBR$ $+RBG - BRG + BGR)$	$\frac{1}{2}(RBG - GBR + BRG$ $-BGR)$
7	$\frac{1}{\sqrt{2}}(RBB - BRB)$	$\frac{1}{\sqrt{6}}(RBB + BRB - 2BBR)$
8	$\frac{1}{\sqrt{2}}(GBB - BGB)$	$\frac{1}{\sqrt{6}}(GBB + BGB - 2BBG)$

2.1.2 Wave Functions of the Quark-antiquark Pair

The quark-antiquark pair color must be $[111]_C$ and $[21]_C$ configurations for heavy quark-antiquark pair ($c\bar{c}$). The spin wave functions of mesons can be singlet (S = 0) or triplet (S = 1). In this part, we worked out and listed all configurations of $c\bar{c}$ ground state that corresponds to the q^3 part in Table 2.9. Moreover, the configuration of spin and color are also worked out and shown in Table 2.10 and 2.11. The $c\bar{c}$ color wave function was the conjugation of the q^3 or baryon color wave function. The anti-color can be represented in the [11] pattern in group theory language as

$$\bar{R} = \frac{1}{\sqrt{2}}(GB - BG),\ \bar{G} = \frac{1}{\sqrt{2}}(BR - RB),\ \bar{B} = \frac{1}{\sqrt{2}}(RG - GR). \tag{2.15}$$

For example, the color singlet of baryon can be changed to color singlet of meson.

$$\begin{aligned}\psi^C_{[111],c\bar{c}} &= (RGB - RBG + GBR - GRB + BRG - BGR)^\dagger \\ &= (R(GB - BG))^\dagger + (G(BR - RB))^\dagger + (B(RG - GR))^\dagger \\ &= R\bar{R} + G\bar{G} + B\bar{B} \\ \Rightarrow &= \frac{1}{\sqrt{3}}(R\bar{R} + G\bar{G} + B\bar{B}).\end{aligned} \tag{2.16}$$

Table 2.9 The wave function of $c\bar{c}$ part.

color singlet model	$\psi^O_{[3]}\psi^C_{[111]}\chi_1\phi_{[c\bar{c}]}$
	$\psi^O_{[3]}\psi^C_{[111]}\chi_0\phi_{[c\bar{c}]}$
color octet model	$\psi^O_{[3]}\psi^C_{[21]}\chi_1\phi_{[c\bar{c}]}$
	$\psi^O_{[3]}\psi^C_{[21]}\chi_0\phi_{[c\bar{c}]}$

Table 2.10 Spin wave functions of meson.

Types	Spin(χ_{S,S_3})
Triplet	$\chi_{1,1} = \|\uparrow\uparrow\rangle$
	$\chi_{1,0} = \frac{1}{\sqrt{2}}\|\uparrow\downarrow + \uparrow\downarrow\rangle$
	$\chi_{1,-1} = \|\downarrow\downarrow\rangle$
Singlet	$\chi_{0,0} = \frac{1}{\sqrt{2}}\|\uparrow\downarrow - \uparrow\downarrow\rangle$

Table 2.11 Color wave function of meson.

Color list	$Q\bar{Q}$
Singlet	$\frac{1}{\sqrt{3}}(R\bar{R} + G\bar{G} + B\bar{B})$
Octet	
1	$B\bar{R}$
2	$B\bar{G}$
3	$-G\bar{R}$
4	$\frac{1}{\sqrt{2}}(R\bar{R} - G\bar{G})$
5	$R\bar{G}$
6	$\frac{1}{\sqrt{6}}(2B\bar{B} - R\bar{R}$ $-G\bar{G})$
7	$-G\bar{B}$
8	$R\bar{B}$

2.1.3 Total Wave Functions of the P_c

We show all configurations of P_c in Table 2.12 by combining q^3 part of Table 2.4 and $c\bar{c}$ part of Table 2.9. In Table 2.12, we define the configuration in short form to simplify the following discussion. We assume that the particles are in their ground state and therefore the spatial part is a totally symmetric wave function and not included in the short form. From the direct product between q^3 and quark-antiquark ($c\bar{c}$) parts, the configurations of P_c can generate the states in the different quantum number of each configuration, where I is the total isospin and J is the total spin. It can be following in Eq. (2.6) and (2.12) which included with the spatial-spin-flavor configurations and spin-flavor configurations in Tables 2.1, 2.2, 2.3, and 2.5. We define $\psi^{O}_{[3]}$ as the symmetric state of spatial part or ground state. $\phi_{[3]}$ and $\chi_{[3]}$ are symmetric wave functions of flavor (ϕ_S) and spin (χ_S), respectively. $\phi_{[21]}$ and $\chi_{[21]}$ are mixed symmetric wave functions of flavor (ϕ_λ and ϕ_ρ) and spin (χ_λ andχ_ρ), respectively.

Table 2.12 All configuration of P_c with the short form and possible quantum numbers.

Short form	Configuration q^3 part		Configuration $c\bar{c}$ part	I	J
$C[111]\ F[3]\ S[3]\ [\chi_1]$	$\psi^O_{[3]}\psi^C_{[111]}\phi_{[3]}\chi_{[3]}$	$\otimes$	$\psi^O_{[3]}\psi^C_{[111]}\phi(c\bar{c})\chi_1$	$\frac{3}{2}$	$\frac{1}{2},\frac{3}{2},\frac{5}{2}$
$C[111]\ F[3]\ S[3]\ [\chi_0]$	$\psi^O_{[3]}\psi^C_{[111]}\phi_{[3]}\chi_{[3]}$	$\otimes$	$\psi^O_{[3]}\psi^C_{[111]}\phi(c\bar{c})\chi_0$	$\frac{3}{2}$	$\frac{3}{2}$
$C[111]\ F[21]\ S[21]\ [\chi_1]$	$\psi^O_{[3]}\psi^C_{[111]}\phi_{[21]}\chi_{[21]}$	$\otimes$	$\psi^O_{[3]}\psi^C_{[111]}\phi(c\bar{c})\chi_1$	$\frac{1}{2}$	$\frac{1}{2},\frac{3}{2}$
$C[111]\ F[21]\ S[21]\ [\chi_0]$	$\psi^O_{[3]}\psi^C_{[111]}\phi_{[21]}\chi_{[21]}$	$\otimes$	$\psi^O_{[3]}\psi^C_{[111]}\phi(c\bar{c})\chi_0$	$\frac{1}{2}$	$\frac{1}{2}$
$C[21]\ F[3]\ S[21]\ [\chi_1]$	$\psi^O_{[3]}\psi^C_{[21]}\phi_{[3]}\chi_{[21]}$	$\otimes$	$\psi^O_{[3]}\psi^C_{[21]}\phi(c\bar{c})\chi_1$	$\frac{3}{2}$	$\frac{1}{2},\frac{3}{2}$
$C[21]\ F[3]\ S[21]\ [\chi_0]$	$\psi^O_{[3]}\psi^C_{[21]}\phi_{[3]}\chi_{[21]}$	$\otimes$	$\psi^O_{[3]}\psi^C_{[21]}\phi(c\bar{c})\chi_0$	$\frac{3}{2}$	$\frac{1}{2}$
$C[21]\ F[21]\ S[3]\ [\chi_1]$	$\psi^O_{[3]}\psi^C_{[21]}\phi_{[21]}\chi_{[3]}$	$\otimes$	$\psi^O_{[3]}\psi^C_{[21]}\phi(c\bar{c})\chi_1$	$\frac{1}{2}$	$\frac{1}{2},\frac{3}{2},\frac{5}{2}$
$C[21]\ F[21]\ S[3]\ [\chi_0]$	$\psi^O_{[3]}\psi^C_{[21]}\phi_{[21]}\chi_{[3]}$	$\otimes$	$\psi^O_{[3]}\psi^C_{[21]}\phi(c\bar{c})\chi_0$	$\frac{1}{2}$	$\frac{3}{2}$
$C[21]\ F[21]\ S[21]\ [\chi_1]$	$\psi^O_{[3]}\psi^C_{[21]}\phi_{[21]}\chi_{[21]}$	$\otimes$	$\psi^O_{[3]}\psi^C_{[21]}\phi(c\bar{c})\chi_1$	$\frac{1}{2}$	$\frac{1}{2},\frac{3}{2}$
$C[21]\ F[21]\ S[21]\ [\chi_0]$	$\psi^O_{[3]}\psi^C_{[21]}\phi_{[21]}\chi_{[21]}$	$\otimes$	$\psi^O_{[3]}\psi^C_{[21]}\phi(c\bar{c})\chi_0$	$\frac{1}{2}$	$\frac{1}{2}$
$C[21]\ F[111]\ S[21]\ [\chi_1]$	$\psi^O_{[3]}\psi^C_{[21]}\phi_{[111]}\chi_{[21]}$	$\otimes$	$\psi^O_{[3]}\psi^C_{[21]}\phi(c\bar{c})\chi_1$	0	$\frac{1}{2},\frac{3}{2}$
$C[21]\ F[111]\ S[21]\ [\chi_0]$	$\psi^O_{[3]}\psi^C_{[21]}\phi_{[111]}\chi_{[21]}$	$\otimes$	$\psi^O_{[3]}\psi^C_{[21]}\phi(c\bar{c})\chi_0$	0	$\frac{1}{2}$

We neglected the configuration $C[21]F[111]S[21][\chi_1]$ and $C[21]F[111]S[21][\chi_0]$ since the P_c has no s quark. Thus, the total pentaquark states are 17 states that are listed in this thesis.

The total wave function of pentaquark can take the form as

$$\begin{aligned}
&|\psi^O_{[\lambda],q^3}\psi^C_{[\lambda],q^3}\phi_{[\lambda],q^3}\chi_{[\lambda],q^3}\rangle \otimes |\psi^O_{[\lambda],c\bar{c}}\psi^C_{[\lambda],c\bar{c}}\phi(c\bar{c})\chi_{c\bar{c}}\rangle \\
&= |\psi^O_{[\lambda],q^3} \otimes \psi^O_{[\lambda],c\bar{c}}\rangle\, |\psi^C_{[\lambda],q^3} \otimes \psi^C_{[\lambda],c\bar{c}}\rangle\, |\phi_{[\lambda],q^3} \otimes \phi_{c\bar{c}}\rangle\, |\chi_{[\lambda],q^3} \otimes \chi_{c\bar{c}}\rangle \\
&= |\psi^O_{P_c}\rangle\, |\psi^C_{P_c}\rangle\, |\phi_{([\lambda],P_c}\rangle\, |[\lambda],\chi_{c\bar{c}},jm)\rangle_{P_c}\,,
\end{aligned} \tag{2.17}$$

with

$$
\begin{aligned}
|[\lambda], \chi_{c\bar{c}}, jm)\rangle_{P_c} &= \chi_{P_c}(j,m) \\
&= \sum_{m_1=-j_1}^{j_1} \sum_{m_2=-j_2}^{j_2} CG((j_1 j_2)j; (m_1 m_2)m)\chi_{q^3(j_1,m_1)}\chi_{c\bar{c}(j_2,m_2)},
\end{aligned}
\tag{2.18}
$$

where $[\lambda]$ is Young tabloid representation as $[3]$, $[21]$ and $[111]$, which are the types of q^3 part in pentaquark wave function. The $\chi_{c\bar{c}}$ can either be spin zero or one state. The $\chi_{P_c}(j,m)$ denotes the spin wave function with pair of direct product type as subscript term, j is the total spin, m is spin projection, $\chi_{q^3(j_1,m_1)}$, and $\chi_{c\bar{c}(j_2,m_2)}$ are the spin of baryon part and meson part, and $CG((j_1 j_2)j_3; (m_1 m_2)m_3)$ is the Clebsch-Gordan coefficients.

The representation meaning of $[3]$ denote the quantum number $S = \frac{3}{2}$, $[21]^\lambda$ or $[21]^\rho$ denote the quantum number $S = \frac{1}{2}$ and $[111]$ denote the quantum number $S = 0$.

In the color part, the case of $[111]_C$ is a direct product between the color of q^3 and quark-antiquark pair parts for the pentaquark color singlet. In the case of $[21]_C$, we must sum over all possible color octet product states because each color octet will become the color singlet by the direct product itself. The color singlet of both models can be shown as

For $[111]_C$,

$$
\psi^C_{[222],P_c} = \psi^C_{[111],q^3} \otimes \psi^C_{[111],c\bar{c}} \tag{2.19}
$$

For $[21]_C$,

$$
\psi^C_{[222],P_c} = \frac{1}{\sqrt{8}} \sum_{i=1}^{8} \psi^C_{[21]_i,q^3} \otimes \psi^C_{[21]_i,c\bar{c}} \tag{2.20}
$$

where i is a number of q^3 and $Q\bar{Q}$ color octet states.

We concluded the color wave functions for q^3 and $Q\bar{Q}$ in Table 2.13.

Table 2.13 Color wave function of baryon and meson for pentaquark.

	q^3		$Q\bar{Q}$
Singlet	$\frac{1}{\sqrt{6}}(RGB - RBG + GBR - GRB + BRG - BGR)$		$\frac{1}{\sqrt{3}}(R\bar{R} + G\bar{G} + B\bar{B})$
	$q^3\rho$ type	$q^3\lambda$ type	$Q\bar{Q}$
Octet			
1	$\frac{1}{\sqrt{2}}(RGR - GRR)$	$\frac{1}{\sqrt{6}}(RRG - RGR - GRR)$	$B\bar{R}$
2	$\frac{1}{\sqrt{2}}(RGG - GRG)$	$\frac{1}{\sqrt{6}}(RGG - GRG - 2GGR)$	$B\bar{G}$
3	$\frac{1}{\sqrt{2}}(RBR - BRR)$	$\frac{1}{\sqrt{6}}(2RRB - RBR - BRR)$	$-G\bar{R}$
4	$\frac{1}{2}(RBG + GBR - BRG - BGR)$	$\frac{1}{\sqrt{12}}(2RGB + 2GRB - GBR - RBG - BRG - BGR)$	$\frac{1}{\sqrt{2}}(R\bar{R} - G\bar{G})$
5	$\frac{1}{\sqrt{2}}(GBG - BGG)$	$\frac{1}{\sqrt{6}}(2GGB - GBG - BGG)$	$R\bar{G}$
6	$\frac{1}{\sqrt{12}}(2RGB - 2GRB - GBR + RBG - BRG + BGR)$	$\frac{1}{2}(RBG - GBR + BRG - BGR)$	$\frac{1}{\sqrt{6}}(2B\bar{B} - R\bar{R} - G\bar{G})$
7	$\frac{1}{\sqrt{2}}(RBB - BRB)$	$\frac{1}{\sqrt{6}}(RBB + BRB - 2BBR)$	$-G\bar{B}$
8	$\frac{1}{\sqrt{2}}(GBB - BGB)$	$\frac{1}{\sqrt{6}}(GBB + BGB - 2BBG)$	$R\bar{B}$

2.2 Wave Functions for Decay Channels

The final particles are baryons and mesons which could either be $[qqq]$ and $[c\bar{c}]$ or $[qqc]$ and $[q\bar{c}]$, but only color singlet states. We denote the final particle $[qqq]$ $[c\bar{c}]$ as hidden charm decay channels and $[qqc]$ $[q\bar{c}]$ as open charm decay channels. In the case of a hidden charm channel, the hadron wave function can be taken from the q^3 part and quark-antiquark pair part in the pentaquark wave function. We obtain the baryon wave functions in the following form

$$\Psi_{[111]}(q^3) = \psi^{O}_{[3]}\psi^{C}_{[111]}\psi^{SF}_{[3],q^3} \tag{2.21}$$

$$\Psi_{[111]}(q^2c) = \psi^{O}_{[3]}\psi^{C}_{[111]}\psi^{SF}_{[2],q^2} \otimes \psi^{SF}_{c} \tag{2.22}$$

For the baryon wave function, we can follow the combination ψ^{SF} in Table 2.3 for q^3 and Table 2.14 for q^2c. The flavor wave function for q^3 and q^2c can be expanded according to Table 2.6 and Table 2.15, respectively. In terms of spin and color wave function, both configurations are also the same as in Tables 2.7 and 2.8, respectively.

Table 2.14 The configuration of spin-flavor wave function for open charm baryon.

$[2]_{FS}$	$[2]_F \otimes [2]_S$	$[11]_F \otimes [11]_S$
$[11]_{FS}$	$[2]_F \otimes [11]_S$	$[11]_F \otimes [2]_S$

Table 2.15 Flavor wave function of open charm baryon.

Types	Flavor (ϕ_{I,I_3})
Symmetric ($\phi_{S,c}$)	$\phi_{1,1} = uuc$
	$\phi_{1,0} = \frac{1}{\sqrt{2}}(udc + duc)$
	$\phi_{1,-1} = ddc$
Antisymmetric ($\phi_{A,c}$)	$\phi_{0,0} = \frac{1}{\sqrt{2}}(udc - duc)$

The full wave function of baryons for both configurations is given in Table 2.16.

Table 2.16 Full wave function of baryons.

flavor configuration	Particle	wave function
qqq	Δ	$\psi^O_{[3]}\psi^C_{[111]}\chi_{[3]}\phi_{[3]}$
	p	$\psi^O_{[3]}\psi^C_{[111]}\chi_{[21]}\phi_{[21]}$
qqc	Σ^*	$\psi^O_{[3]}\psi^C_{[111]}\chi_{[3]}\phi_{([2]}$
	Σ	$\psi^O_{[3]}\psi^C_{[111]}\chi_{[21]_\lambda}\phi_{[2]}$
	Λ	$\psi^O_{[3]}\psi^C_{[111]}\chi_{[21]_\rho}\phi_{[11]}$

The wave function of meson are given in Table 2.17. The spin and color wave function provided in the Tables 2.10 and 2.11, respectively.

Table 2.17 Full wave function of mesons.

flavor configuration	Particle	wave function
$c\bar{c}$	J/ψ	$\psi^O_{[3]}\psi^C_{[111]}\chi_1\psi^F_{[c\bar{c}]}$
	η_c	$\psi^O_{[3]}\psi^C_{[111]}\chi_0\phi_{[c\bar{c}]}$
$q\bar{c}$	$\bar{D}^*$	$\psi^O_{[3]}\psi^C_{[111]}\chi_1\phi_{[q\bar{c}]}$
	$\bar{D}$	$\psi^O_{[3]}\psi^C_{[111]}\chi_0\phi_{[q\bar{c}]}$

2.3 Spatial Wave Function of Hadrons

From quantum chromodynamics (QCD), we expect confinement at low energies. Thus, we approximate spatial wave functions by a harmonic oscillator. Furthermore, the harmonic oscillator wave functions can serve as a complete basis of the multiquark wave function. The explicit form is derived from the non-relativistic Schr$\ddot{o}$dinger equation with the Hamiltonian of the N-quark system as

$$H = \sum_{i=1}^{N} \frac{p_i^2}{2m_i} + C\sum_{i<j}^{N}(\vec{r_i} - \vec{r_j})^2. \tag{2.23}$$

After introducing Jacobi coordinates, the complete Hamiltonian reads

$$H_{Q^2} = \frac{{p_\rho}^2}{2m} + C(\rho^2), \tag{2.24}$$

$$H_{q^3} = \frac{{p_\lambda}^2}{2m} + \frac{{p_\rho}^2}{2m} + 3C(\lambda^2 + \rho^2), \tag{2.25}$$

$$H_{q^3Q^2} = \frac{{p_\lambda}^2}{2m} + \frac{{p_\rho}^2}{2m} + \frac{{p_\sigma}^2}{2M} + \frac{\vec{p_\chi}^2}{2u_\chi} + 5C(\lambda^2 + \rho^2 + \sigma^2 + \chi^2), \tag{2.26}$$

where

$$\vec{\rho} = \frac{1}{\sqrt{2}}(\vec{r}_1 - \vec{r}_2), \tag{2.27}$$

$$\vec{\lambda} = \frac{1}{\sqrt{6}}(\vec{r}_1 + \vec{r}_2 - 2\vec{r}_3), \tag{2.28}$$

$$\vec{\sigma} = \frac{1}{\sqrt{2}}(\vec{r}_4 - \vec{r}_5), \tag{2.29}$$

$$\vec{\chi} = \frac{1}{\sqrt{30}}(2(\vec{r}_1 + \vec{r}_2 + \vec{r}_3) - 3(\vec{r}_4 + \vec{r}_5)), \tag{2.30}$$

$$\vec{p}_\rho = \frac{1}{\sqrt{2}}(\vec{p}_1 - \vec{p}_2), \tag{2.31}$$

$$\vec{p}_\lambda = \frac{1}{\sqrt{6}}(\vec{p}_1 + \vec{p}_2 - 2\vec{p}_3), \tag{2.32}$$

$$\vec{p}_\sigma = \frac{1}{\sqrt{2}}(\vec{p}_4 - \vec{p}_5), \tag{2.33}$$

$$\vec{p}_\chi = \frac{\sqrt{5}}{\sqrt{6}}\left(\frac{2M(\vec{p}_1 + \vec{p}_2 + \vec{p}_3) - 3m(\vec{p}_4 + \vec{p}_5)}{3m + 2M}\right), \tag{2.34}$$

$$u_\chi = \frac{5mM}{3m + 2M}, \tag{2.35}$$

where $\vec{p}_1$, $\vec{p}_2$, $\vec{p}_3$, $\vec{p}_4$, and $\vec{p}_5$ are the momenta of quarks, $\vec{r}_1$, $\vec{r}_2$, $\vec{r}_3$, $\vec{r}_4$, and $\vec{r}_5$ are position coordinates of quarks. C is the coupling constant. m and M are the mass of light quark(q) and heavy quark(Q), respectively.

The ground state wave functions in momentum space can be written as

$$\psi^O_{Q^2} = N \exp\left[\frac{-R_M^2}{8}(\vec{p}_{i'} - \vec{p}_{j'})^2\right], \tag{2.36}$$

$$\psi^O_{q^3} = N' \exp\left[\frac{-R_B^2}{2}\left(\left(\frac{\vec{p}_j - \vec{p}_k}{\sqrt{2}}\right)^2 + \left(\frac{\vec{p}_j + \vec{p}_k - 2\vec{p}_i}{\sqrt{6}}\right)^2\right)\right], \tag{2.37}$$

$$\begin{aligned}\psi^O_{q^3Q^2} =& N'' \exp\left[\frac{-R_{q^3}^2}{2}\left(\left(\frac{\vec{p}_1 - \vec{p}_2}{\sqrt{2}}\right)^2 + \left(\frac{\vec{p}_1 + \vec{p}_2 - 2\vec{p}_3}{\sqrt{6}}\right)^2\right)\right] \\ & \exp\left[\frac{-R^2}{2}\left(\frac{\sqrt{5}}{\sqrt{6}}.\frac{2M(\vec{p}_1 + \vec{p}_2 + \vec{p}_3) - 3m(\vec{p}_4 + \vec{p}_5)}{3m + 2M}\right)^2\right] \\ & \exp\left[\frac{-R_{Q^2}^2}{2}\left(\frac{\vec{p}_4 - \vec{p}_5}{\sqrt{2}}\right)^2\right],\end{aligned} \tag{2.38}$$

where N, N', and N'' are the normalization constants. These wave function will be used for calculating the decay probability which is discussed in the next chapter.

CHAPTER III

DECAY CHANNELS OF P_C

In this chapter, we describe the method to obtain the transition amplitude of open channels of P_c states that were constructed in the previous chapter. It was employed to describe the decay processes by considering quark contents. The possible decay processes must follow the OZI rule, which states that a Feynman diagram is suppressed when the transition from the initial to the final state could be separated without cutting a quark line (Le Yaouanc et al., 1988). In this work, we consider the compact pentaquark decay. It has two possible decay processes with different final states. The decay processes are shown in Figures 3.1 and 3.2.

Figure 3.1 The direct decay process diagram.

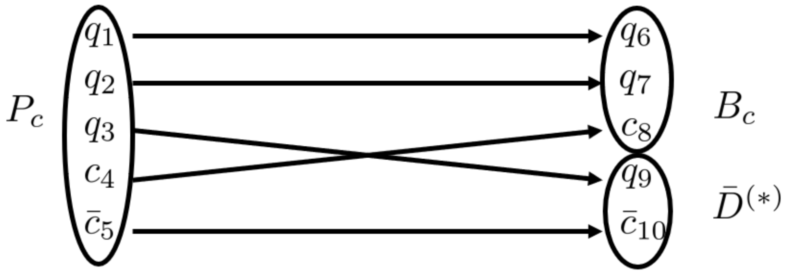

Figure 3.2 The cross decay process diagram.

3.1 Transition Amplitudes

The transition amplitude between pentaquark and final states (baryon and meson) is

$$T = \langle \psi_{final} | \hat{O} | \psi_{initial} \rangle , \tag{3.1}$$

where $\hat{O}$ denote the operator associated with the transition amplitude. For our work, the operator $\hat{O}$ takes the form as,

$$O_d = \lambda_1 \delta^3(\vec{q}_1 - \vec{q}_6)\delta^3(\vec{q}_2 - \vec{q}_7)\delta^3(\vec{q}_3 - \vec{q}_8)\delta^3(\vec{q}_4 - \vec{q}_9)\delta^3(\vec{q}_5 - \vec{q}_{10}), \tag{3.2}$$

$$O_c = \lambda_2 \delta^3(\vec{q}_1 - \vec{q}_6)\delta^3(\vec{q}_2 - \vec{q}_7)\delta^3(\vec{q}_3 - \vec{q}_9)\delta^3(\vec{q}_4 - \vec{q}_8)\delta^3(\vec{q}_5 - \vec{q}_{10}), \tag{3.3}$$

where d and c stand for direct diagram and cross diagram, respectively.

From Eqs. (2.17) and (2.18), we obtain the states of P_c as

$$\begin{aligned} |\Psi\rangle_{P_c} = \sum_{m_1=-j_1}^{j_1} \sum_{m_2=-j_2}^{j_2} & CG((j_1 j_2)j;(m_1 m_2)m) \, |\psi^O_{P_c}\rangle \, |\psi^C_{P_c}\rangle \, |\phi_{([\lambda],P_c}\rangle \\ & |\chi_{q^3(j_1,m_1)}\rangle \, |\chi_{c\bar{c}(j_2,m_2)}\rangle \, . \end{aligned} \tag{3.4}$$

For the final particle, the baryon and meson wave functions can be separated by considering the decays diagram as shown in Figures 3.1 and 3.2:

1. The direct decay process diagram, the q^3 baryon is formed as

$$|\Psi\rangle_B = |\psi^O_B\rangle \, |\psi^C_{[111]}\rangle \, |\phi_{([\lambda])}\rangle \, |\chi_{([\lambda])}\rangle \, , \tag{3.5}$$

where $[\lambda]$ ([3] or [21]) in the flavor and the spin part of final baryon q^3 must be the same type to get the total symmetric spin-flavor wave function.

The final mesons are

$$|\Psi\rangle_M = |\psi^O_M\rangle \, |\psi^C_{[111]}\rangle \, |\phi(c\bar{c})\rangle \, |\chi\rangle \, , \tag{3.6}$$

where χ can either be spin zero and spin one state which are given in Table 2.10.

Thus, the final particle obtains the direct product form as

$$\begin{aligned}
|\Psi\rangle_1 &= |\psi_{Baryon}\psi_{Meson}\rangle \\
&= |\psi_B^O\psi_{[111]}^C\phi_{([\lambda],q^3)}\chi_{([\lambda],q^3)}\rangle\,|\psi_M^O\psi_{[111]}^C\phi_{c\bar{c}}\chi\rangle \\
&= |\psi_B^O\psi_M^O\rangle\,|\psi_{[111]B,M}^C\rangle\,|\phi_{([\lambda],q^3)c\bar{c}}\rangle\,|\chi_{([\lambda],q^3)}\otimes\chi\rangle \\
&= \sum_{m_1=-j_1}^{j_1}\sum_{m_2=-j_2}^{j_2} CG((j_1j_2)j;(m_1m_2)m) \\
&\quad |\chi_{B(j_1,m_1)}\rangle_f\,|\chi_{M(j_2,m_2)}\rangle\,|\psi_B^O\psi_M^O\rangle\,|\psi_{[111]B,M}^C\rangle\,|\phi_{([\lambda],q^3)c\bar{c}}\rangle\,. \qquad (3.7)
\end{aligned}$$

2. The cross decay process diagram reads

$$|\Psi\rangle_B = |\psi_B^O\rangle\,|\psi_{[111]}^C\rangle\,|\phi_{([\lambda],q^2)c}\rangle\,|\chi_{([\lambda],q^2)c}\rangle\,, \qquad (3.8)$$

where $[\lambda]$ ($[2]$ or $[11]$) in flavor and spin part of final baryon q^2c must be the same to get the total symmetric spin-flavor wave function.

The meson in the final state are

$$|\Psi\rangle_M = |\psi_M^O\rangle\,|\psi_{[111]}^C\rangle\,|\phi_{q\bar{c}}\rangle\,|\chi\rangle\,. \qquad (3.9)$$

Thus, the final particle can get the direct product form as

$$\begin{aligned}
|\Psi\rangle_1 &= |\psi_{Baryon}\psi_{Meson}\rangle \\
&= |\psi_B^O\psi_{[111]}^C\phi_{([\lambda],q^3)}\chi_{([\lambda],q^3)}\rangle\,|\psi_M^O\psi_{[111]}^C\phi_{c\bar{c}}\chi\rangle \\
&= |\psi_B^O\psi_M^O\rangle\,|\psi_{[111]B,M}^C\rangle\,|\phi_{([\lambda],q^3)c\bar{c}}\rangle\,|\chi_{([\lambda],q^3)}\otimes\chi\rangle \\
&= \sum_{m_1=-j_1}^{j_1}\sum_{m_2=-j_2}^{j_2} CG((j_1j_2)j;(m_1m_2)m) \\
&\quad |\chi_{B(j_1,m_1)}\rangle_f\,|\chi_{M(j_2,m_2)}\rangle\,|\psi_B^O\psi_M^O\rangle\,|\psi_{[111]B,M}^C\rangle\,|\phi_{([\lambda],q^3)c\bar{c}}\rangle \qquad (3.10)
\end{aligned}$$

2. The cross decay process diagram reads

$$|\Psi\rangle_B = |\psi_B^O\rangle \, |\psi_{[111]}^C\rangle \, |\phi_{([\lambda],q^2)c}\rangle \, |\chi_{([\lambda],q^2)c}\rangle \, , \tag{3.11}$$

where $[\lambda]$ ($[2]$ *or* $[11]$) in flavor and spin part of final baryon q^2c must be the same to get the total symmetric spin-flavor wave function.

The meson in the final state are

$$|\Psi\rangle_M = |\psi_M^O\rangle \, |\psi_{[111]}^C\rangle \, |\phi_{q\bar{c}}\rangle \, |\chi\rangle \, . \tag{3.12}$$

Thus, the final particle can get the direct product form as

$$\begin{aligned}
|\Psi\rangle_2 &= |\psi_{Baryon}\psi_{Meson}\rangle \\
&= |\psi_B^O \psi_{[111]}^C \phi_{([\lambda],q^2)c} \chi_{([\lambda],q^2)c}\rangle \, |\psi_M^O \psi_{[111]}^C \phi_{q\bar{c}} \chi\rangle \\
&= |\psi_B^O \psi_M^O\rangle \, |\psi_{[111]B,M}^C\rangle \, |\phi_{([\lambda],q^2)c} \otimes \phi_{q\bar{c}}\rangle \, |\chi_{([\lambda],q^2c)} \otimes \chi\rangle \\
&= |\psi_B^O \psi_M^O\rangle_f \, |\psi_{[111]B,M}^C\rangle \, \langle \phi_{([\lambda],q^3)c\bar{c}} | \phi_{([\lambda],q^2)c} \otimes \phi_{q\bar{c}}\rangle \, |\phi_{([\lambda],q^3)c\bar{c}}\rangle \\
&\quad \langle \chi_{([\lambda],q^3)} \otimes \chi | \chi_{([\lambda],q^2)c} \otimes \chi_{q\bar{c}}\rangle \, |\chi_{([\lambda],q^3)} \otimes \chi\rangle \\
&= \sum_{m_1=-j_1}^{j_1} \sum_{m_2=-j_2}^{j_2} CG((j_1 j_2)j;(m_1 m_2)m) \, |\chi_{B(j_1,m_1)}\rangle \, |\chi_{M(j_2,m_2)}\rangle \\
&\quad |\psi_B^O \psi_M^O\rangle \, |\psi_{[111]B,M}^C\rangle \, \langle \phi_{([\lambda],q^3)c\bar{c}} | \phi_{([\lambda],q^2)c} \otimes \phi_{q\bar{c}}\rangle \, |\phi_{([\lambda],q^3)c\bar{c}}\rangle \\
&\quad \langle \chi_{([\lambda],q^3)} \otimes \chi | \chi_{([\lambda],q^2)c} \otimes \chi_{q\bar{c}}\rangle \, .
\end{aligned} \tag{3.13}$$

Due to the calculation of the inner product with initial state and final state, we can employ the Wigner's 9-j symbols in Appendix C to find the coefficient of $\langle \phi_{([\lambda],q^3)c\bar{c}} | \phi_{([\lambda],q^2)c} \otimes \phi_{q\bar{c}}\rangle$ and $\langle \chi_{([\lambda],q^3)} \otimes \chi | \chi_{([\lambda],q^2)c} \otimes \chi_{q\bar{c}}\rangle$.

From Eq. (3.1), we obtain the transition amplitude of both diagrams by using the wave function in Eqs. (3.4), (3.10) and (3.13). For the direct decay process, the transition amplitude is

$$T_1 = \langle \psi^O_B \psi^O_M | \, O_i \, | \psi^O_{P_c} \rangle \, \langle \psi^C_{[111]B,M} | \psi^C_{P_c} \rangle \, \langle \phi_{([\lambda],q^3)c\bar{c}_f} | \phi_{([\lambda],q^3)c\bar{c}_i} \rangle$$
$$\sum_{m_1=-j_1}^{j_1} \sum_{m_2=-j_2}^{j_2} \sum_{m'_1=-j'_1}^{j'_1} \sum_{m'_2=-j'_2}^{j'_2} CG((j_1 j_2)j;(m_1 m_2)m) \, CG((j'_1 j'_2)j';(m'_1 m'_2)m')$$
$$\langle \chi_{B(j'_1,m'_1)} | \chi_{B(j_1,m_1)} \rangle \, \langle \chi_{M(j'_2,m'_2)} | \chi_{M(j_2,m_2)} \rangle \, . \tag{3.14}$$

The transition amplitude for the cross decay process is evaluated as

$$T_2 = \langle \psi^O_B \psi^O_M | \, O_i \, | \psi^O_{P_c} \rangle \, \langle \psi^C_{[111]B,M} | \psi^C_{P_c} \rangle \, \langle \phi_{([\lambda],q^3)c\bar{c}_f} | \phi_{([\lambda],q^3)c\bar{c}_i} \rangle$$
$$\sum_{m_1=-j_1}^{j_1} \sum_{m_2=-j_2}^{j_2} \sum_{m'_1=-j'_1}^{j'_1} \sum_{m'_2=-j'_2}^{j'_2} CG((j_1 j_2)j;(m_1 m_2)m) \, CG((j'_1 j'_2)j';(m'_1 m'_2)m')$$
$$\langle \chi_{B(j'_1,m'_1)} | \chi_{B(j_1,m_1)} \rangle \, \langle \chi_{M(j'_2,m'_2)} | \chi_{M(j_2,m_2)} \rangle$$
$$\langle \chi_{([\lambda],q^3)} \otimes \chi_{[1 \, or \, 0]} | \chi_{([\lambda],q^2)c} \otimes \chi_{q\bar{c}} \rangle \, \langle \phi_{([\lambda],q^3)c\bar{c}} | \phi_{([\lambda],q^2)c} \otimes \phi_{q\bar{c}} \rangle \, . \tag{3.15}$$

3.2 Spin-Flavor-Color Transition Amplitude

In this section, the spin-flavor-color transition amplitude is calculated to find the possible channels. We employ the wave functions of P_c and final states which are discussed in the previous section to determine the transition amplitude which were evaluated and provided in Tables 3.1 and 3.2 with isospin $\frac{3}{2}$ and $\frac{1}{2}$, respectively. In these tables, $C[\lambda]$ is the type of color product of pentaquark. $F[\lambda]$, and $S[\lambda]$ are the q^3 configurations of flavor and spin. $[\chi_1]$ and $[\chi_0]$ are the spin of $c\bar{c}$. The transition amplitudes in Eqs. (3.14) and (3.15) are calculated.

Table 3.1 The allowed spin-flavor-color transition amplitudes for I = 3/2 of pentaquark.

P_c Configuration	J^P	$\Delta\eta_c$	$\Delta J/\psi$	$\Sigma_c^*\bar{D}$	$\Sigma_c\bar{D}$	$\Sigma_c^*\bar{D}^*$	$\Sigma_c\bar{D}^*$
$C[111]F[3]S[3][\chi_1]$	$\frac{5}{2}^-$		1			$\frac{1}{3}$	
$C[111]F[3]S[3][\chi_1]$	$\frac{3}{2}^-$		1	$\frac{\sqrt{\frac{5}{3}}}{6}$		$\frac{1}{8}$	$\frac{\sqrt{5}}{9}$
$C[111]F[3]S[3][\chi_0]$	$\frac{3}{2}^-$		1	$\frac{1}{6}$		$\frac{\sqrt{\frac{5}{3}}}{6}$	$-\frac{1}{3\sqrt{3}}$
$C[111]F[3]S[3][\chi_1]$	$\frac{1}{2}^-$	1			$\frac{\sqrt{\frac{2}{3}}}{3}$	$-\frac{1}{9}$	$\frac{\sqrt{2}}{9}$
$C[21]F[3]S[21][\chi_1]$	$\frac{3}{2}^-$			$\frac{2}{3\sqrt{3}}$		$-\frac{2\sqrt{5}}{9}$	$-\frac{2}{9}$
$C[21]F[3]S[21][\chi_1]$	$\frac{1}{2}^-$				$\frac{1}{3\sqrt{3}}$	$-\frac{2\sqrt{2}}{9}$	$-\frac{5}{9}$
$C[21]F[3]S[21][\chi_0]$	$\frac{1}{2}^-$				$-\frac{1}{3}$	$-\frac{2\sqrt{\frac{2}{3}}}{3}$	$\frac{1}{3\sqrt{3}}$

Table 3.2 The allowed spin-flavor-color transition amplitudes for total I = 1/2 of pentaquark.

P_c Configuration	J^P	$p\eta_c$	pJ/ψ	$\Sigma_c^*\bar{D}$	$\Sigma_c\bar{D}$	$\Lambda_c\bar{D}$	$\Sigma_c^*\bar{D}^*$	$\Sigma_c\bar{D}^*$	$\Lambda_c\bar{D}^*$
$C[111]F[21]S[21][\chi_1]$	$\frac{3}{2}^-$		1	$-\frac{1}{3\sqrt{6}}$			$\frac{\sqrt{\frac{5}{2}}}{9}$	$\frac{1}{9\sqrt{2}}$	$\frac{1}{3\sqrt{2}}$
$C[111]F[21]S[21][\chi_1]$	$\frac{1}{2}^-$		1		$-\frac{1}{6\sqrt{6}}$	$\frac{1}{2\sqrt{6}}$	$\frac{1}{9}$	$\frac{5}{18\sqrt{2}}$	$-\frac{1}{6\sqrt{2}}$
$C[111]F[21]S[21][\chi_0]$	$\frac{1}{2}^-$	1			$\frac{1}{6\sqrt{2}}$	$\frac{1}{6\sqrt{2}}$	$\frac{1}{3\sqrt{3}}$	$-\frac{1}{6\sqrt{6}}$	$\frac{1}{2\sqrt{6}}$
$C[21]F[21]S[3][\chi_1]$	$\frac{5}{2}^-$						$-\frac{2}{3}$		
$C[21]F[21]S[3][\chi_1]$	$\frac{3}{2}^-$			$-\frac{\sqrt{\frac{5}{3}}}{3}$			$-\frac{1}{9}$	$-\frac{2\sqrt{5}}{9}$	
$C[21]F[21]S[3][\chi_1]$	$\frac{1}{2}^-$				$-\frac{2\sqrt{\frac{2}{3}}}{3}$		$\frac{2}{9}$	$-\frac{2\sqrt{2}}{9}$	
$C[21]F[21]S[3][\chi_0]$	$\frac{3}{2}^-$			$-\frac{1}{3}$			$-\frac{\sqrt{\frac{5}{3}}}{3}$	$\frac{2}{3\sqrt{3}}$	
$C[21]F[21]S[21][\chi_1]$	$\frac{3}{2}^-$			$\frac{\sqrt{\frac{2}{3}}}{3}$			$-\frac{\sqrt{10}}{9}$	$-\frac{\sqrt{2}}{9}$	$\frac{\sqrt{2}}{3}$
$C[21]F[21]S[21][\chi_1]$	$\frac{1}{2}^-$				$\frac{1}{3\sqrt{6}}$	$\frac{1}{\sqrt{6}}$	$-\frac{2}{9}$	$-\frac{5}{9\sqrt{2}}$	$-\frac{1}{3\sqrt{2}}$
$C[21]F[21]S[21][\chi_0]$	$\frac{1}{2}^-$				$-\frac{1}{3\sqrt{2}}$	$\frac{1}{3\sqrt{2}}$	$-\frac{2}{3\sqrt{3}}$	$\frac{1}{3\sqrt{6}}$	$-\frac{1}{\sqrt{6}}$

3.3 Partial Decay Width

The partial decay width for the transition of P_c states to baryon-meson final states can be calculated by Fermi's Golden Rule (in the center of mass frame)

$$\Gamma_{fi} = 2\pi |T_{fi}|^2 \rho(E_f), \tag{3.16}$$

where $\rho(E_f)$ is the density of final state.

$$\Gamma_{P_c \to BM} = (2\pi)^4 \int \frac{d^3p_B}{(2\pi)^3} \frac{d^3p_M}{(2\pi)^3} \delta^{(3)}(\vec{p}_B + \vec{p}_M)\delta(m_{P_c} - E_B - E_M)|T_{f,i}(\vec{q})|^2, \tag{3.17}$$

$$\Gamma_{P_c \to BM} = \frac{1}{(2\pi)^2} \int q^2 dq d\Omega\, \delta(m - E_B - E_M)|T_{f,i}(\vec{q})|^2, \tag{3.18}$$

where m is the P_c mass, $\vec{q}$ is the final momentum, and $E_{B,M} = \sqrt{m_{B,M}^2 + p_{B,M}^2}$ is the energy of the outgoing baryons and mesons with mass $m_{B,M}$ and momentum $\vec{p}_{B,M}$ which is equal $|\vec{q}|$. We can calculate this equation by using the property of δ-function

$$\Gamma_{P_c \to BM} = \frac{|\vec{q}|E_B E_M}{(2\pi)^2 m_{p_c}} \int d\Omega |T_{f,i}(\vec{q})|^2 \,. \tag{3.19}$$

The transition amplitude of the partial decay width for the transition can be written as

$$\Gamma_{P_c \to BM} = Cf(B,M)|\langle \psi_f^{SFC}|\psi_i^{SFC}\rangle|^2, \tag{3.20}$$

where C is a constant, $\langle \psi_f^{SFC}|\psi_i^{SFC}\rangle$ is the transition coefficient between initial and final states, and the function $f(B,M)$ is the kinematical phase-space factor depending on the relative momentum and the masses of baryon and meson. Due to the harmonic oscillator approximation with the particles in ground state, $f(B,M)$ is replaced by the phenomenological function (Vandermeulen, 1988; Gutsche et al., 1997; Gutsche et al., 1999; Srisuphaphon et al., 2016)

$$f(B, M) = \frac{|\vec{q}|E_1E_2}{m_{P_c}} \exp\{-1.2 \text{ GeV}^{-1} (s - s_0)^{1/2}\}, \tag{3.21}$$

with $s_0 = (m_B + m_M)^2$, $|\vec{q}| = \frac{1}{2m_{P_c}}\sqrt{(m_{pc}^2 + (m_B - m_M)^2)(m_{pc}^2 + s_0)}$,
$\sqrt{s} = (m_B^2 + q^2)^{1/2} + (m_M^2 + q^2)^{1/2}$ and $E_1E_2 = \frac{1}{2}(m_{pc}^2 - m_B^2 - m_M^2 - 2q^2)$.

We calculate the phase space factor from Eq. (3.21) by using the initial particles as $P_c(4312)$, $P_c(4440)$ and $P_c(4457)$ with the processes $P_c \to B\eta_c$, $P_c \to BJ/\psi$, $P_c \to B_c\bar{D}$ and $P_c \to B_c\bar{D}^*$. The results of our calculations are listed in Table 3.3.

In Table 3.3, the phase space factor does not allow the $\Sigma_c\bar{D}^*$ and $\Sigma_c^*\bar{D}^*$ channels because the energy of all three P_c are sufficient here. Thus, we need to eliminate these two decay channels for consideration of allowed channels.

Table 3.3 Phase space factor for $P_c(4312)$, $P_c(4440)$ and $P_c(4457)$ with possible processes.

Final particles	Total mass of final particles (GeV)	$P_c(4312)$	$P_c(4440)$	$P_c(4457)$
$p\eta_c$	3.922	0.08056	0.07038	0.06911
$\Delta\eta_c$	4.214	0.12653	0.11442	0.11221
pJ/ψ	4.035	0.08929	0.07827	0.07686
$\Delta J/\psi$	4.327	N/A	0.12631	0.12516
$\Lambda_c\bar{D}$	4.157	0.15350	0.13097	0.12797
$\Sigma_c\bar{D}$	4.325	N/A	0.16237	0.16014
$\Sigma_c^*\bar{D}$	4.390	N/A	0.16176	0.16517
$\Lambda_c\bar{D}^*$	4.297	0.12507	0.16132	0.15847
$\Sigma_c\bar{D}^*$	4.465	N/A	N/A	N/A
$\Sigma_c^*\bar{D}^*$	4.530	N/A	N/A	N/A

3.4 Partial Decay Width Ratios

We can find the normalized partial decay width of states which takes the form

$$\frac{\Gamma_i}{\Gamma_{ref}} = \frac{f(B_i, M_i)|\langle\psi_f^{SFC}|\psi_i^{SFC}\rangle|_i^2}{f(B_{ref}, M_{ref})|\langle\psi_f^{SFC}|\psi_i^{SFC}\rangle|_{ref}^2}, \tag{3.22}$$

where Γ_i is the decay width of arbitrary allowed decay channels and Γ_{ref} is the reference decay width that we choose.

We study the partial decay width ratio for the possible allowed decay channels. In the following tables, the squared transition amplitude of the three experimentally observed P_c ($P_c(4312)$, $P_c(4440)$ and $P_c(4457)$) are given in three sub-rows.

We consider the partial decay width ratio under the conditions as:

1) Choose one mode as the reference channel for each configuration (Shown in Tables 3.4 and 3.5)

2) Choose $P_c(4312) \rightarrow pJ/\psi$ as reference channel for all configurations (Shown in Tables 3.6 and 3.7).

Table 3.4 The partial width ratio results of P_c configuration for $P_c(4312)$, $P_c(4440)$ and $P_c(4457)$ with I = $\frac{3}{2}$.

J^p	P_c configuration	$\Delta J/\psi$	$\Delta\eta_c$	pJ/ψ	$p\eta_c$	$\Sigma_c^*\bar{D}$	$\Sigma_c\bar{D}$	$\Lambda_c\bar{D}$	$\Lambda_c\bar{D}^*$	Total
		N/A								N/A
$\frac{5}{2}^-$	$C[111]F[3]S[3][\chi_1]$	1								1
		1								1
		N/A				N/A				N/A
$\frac{3}{2}^-$	$C[111]F[3]S[3][\chi_1]$	1				0.06				1.06
		1				0.06				1.06
			1			N/A				1
	$C[111]F[3]S[3][\chi_0]$		1			0.04				1.04
			1			0.04				1.04
						N/A				N/A
	$C[21]F[3]S[21][S^*]$					1				1
						1				1

Continued on next page

Table 3.4 The partial width ratio results of P_c configuration for $P_c(4312)$, $P_c(4440)$ and $P_c(4457)$ with I = $\frac{3}{2}$ (Continued).

J^p	P_c configuration	$\Delta J/\psi$	$\Delta\eta_c$	pJ/ψ	$p\eta_c$	$\Sigma_c^*\bar{D}$	$\Sigma_c\bar{D}$	$\Lambda_c\bar{D}$	$\Lambda_c\bar{D}^*$	Total
		N/A					N/A			N/A
$\frac{1}{2}^-$	$C[111]F[3]S[3][\chi_1]$	1					0.10			1.10
		1					0.10			1.10
							N/A			N/A
	$C[21]F[3]S[21][\chi_1]$						1			1
							1			1
							N/A			N/A
	$C[21]F[3]S[21][\chi_0]$						1			1
							1			1

Table 3.5 The partial width ratio results of P_c configuration for $P_c(4312)$, $P_c(4440)$ and $P_c(4457)$ with I = $\frac{1}{2}$.

J^p	P_c configuration	$\Delta J/\psi$	$\Delta\eta_c$	pJ/ψ	$p\eta_c$	$\Sigma_c^*\bar{D}$	$\Sigma_c\bar{D}$	$\Lambda_c\bar{D}$	$\Lambda_c\bar{D}^*$	Total
				1		N/A			0.08	1.08
$\frac{3}{2}^-$	$C[111]F[21]S[21][\chi_1]$			1		0.04			0.12	1.16
				1		0.04			0.11	1.15
						N/A				-
	$C[21]F[21]S[3][\chi_1]$					1				1
						1				1
						N/A				N/A
	$C[21]F[21]S[21][\chi_0]$					1				1
						1				1
						N/A			1	1
	$C[21]F[21]S[21][\chi_1]$					1			2.88	3.88
						1			2.99	3.99

Continued on next page

Table 3.5 The partial width ratio results of P_c configuration for $P_c(4312)$, $P_c(4440)$ and $P_c(4457)$ with I = $\frac{1}{2}$ (Continued).

J^p	P_c configuration	$\Delta J/\psi$	$\Delta\eta_c$	pJ/ψ	$p\eta_c$	$\Sigma_c^*\bar{D}$	$\Sigma_c\bar{D}$	$\Lambda_c\bar{D}$	$\Lambda_c\bar{D}^*$	Total
				1			N/A	0.07	0.02	1.09
$\frac{1}{2}^-$	$C[111]F[21]S[21][\chi_1]$			1			0.01	0.07	0.03	1.11
				1			0.01	0.07	0.03	1.11
					1		N/A	0.03	0.07	1.10
	$C[111]F[21]S[21][\chi_0]$				1		0.03	0.03	0.10	1.16
					1		0.03	0.03	0.10	1.16
							N/A			N/A
	$C[21]F[21]S[3][\chi_1]$						1			1
							1			1
							N/A	1	0.27	1.27
	$C[21]F[21]S[21][\chi_1]$						1	7.19	2.97	11.16
							1	7.26	2.98	11.24

Continued on next page

Table 3.5 The partial width ratio results of P_c configuration for $P_c(4312)$, $P_c(4440)$ and $P_c(4457)$ with I = $\frac{1}{2}$ (Continued).

J^p	P_c configuration	$\Delta J/\psi$	$\Delta\eta_c$	pJ/ψ	$p\eta_c$	$\Sigma_c^*\bar{D}$	$\Sigma_c\bar{D}$	$\Lambda_c\bar{D}$	$\Lambda_c\bar{D}^*$	Total
							N/A	1	2.44	3.44
	$C[21]F[21]S[21][\chi_0]$						1	0.80	2.97	4.77
							1	0.80	2.98	4.78

Table 3.6 The partial width ratio results of P_c configuration with I = $\frac{3}{2}$ for $P_c(4312)$, $P_c(4440)$ and $P_c(4457)$ which are normalized by $P_c(4312) \to pJ/\psi$ as reference channel.

J^p	P_c configuration	$\Delta J/\psi$	$\Delta\eta_c$	pJ/ψ	$p\eta_c$	$\Sigma_c^*\bar{D}$	$\Sigma_c\bar{D}$	$\Lambda_c\bar{D}$	$\Lambda_c\bar{D}^*$	Total
		N/A								N/A
$\frac{5}{2}^-$	$C[111]F[3]S[3][\chi_1]$	1.42								1.42
		1.40								1.40
		N/A				N/A				N/A
$\frac{3}{2}^-$	$C[111]F[3]S[3][\chi_1]$	1.42				0.08				1.50
		1.40				0.09				1.49
			1.42			N/A				1.42
	$C[111]F[3]S[3][\chi_0]$		1.28			0.05				1.33
			1.26			0.05				1.31
						N/A				N/A
	$C[21]F[3]S[21][\chi_1]$					0.27				0.27
						0.27				0.27

Continued on next page

Table 3.6 The partial width ratio results of P_c configuration with I = $\frac{3}{2}$ for $P_c(4312)$, $P_c(4440)$ and $P_c(4457)$ which are normalized by $P_c(4312) \to pJ/\psi$ as reference channel (Continued).

J^p	P_c configuration	$\Delta J/\psi$	$\Delta\eta_c$	pJ/ψ	$p\eta_c$	$\Sigma_c^*\bar{D}$	$\Sigma_c\bar{D}$	$\Lambda_c\bar{D}$	$\Lambda_c\bar{D}^*$	Total
		N/A					N/A			N/A
$\frac{1}{2}^-$	$C[3]F[3]S[3][\chi_1]$	1.42					0.14			1.56
		1.40					0.13			1.53
							N/A			N/A
	$C[21]F[3]S[21][\chi_1]$						0.07			0.07
							0.07			0.07
							N/A			N/A
	$C[21]F[3]S[21][\chi_0]$						0.20			0.20
							0.20			0.20

Table 3.7 The partial width ratio results of P_c configuration with I = $\frac{1}{2}$ for $P_c(4312)$, $P_c(4440)$ and $P_c(4457)$ which are normalized by $P_c(4312) \to pJ/\psi$ as reference channel.

J^p	P_c configuration	$\Delta J/\psi$	$\Delta\eta_c$	pJ/ψ	$p\eta_c$	$\Sigma_c^*\bar{D}$	$\Sigma_c\bar{D}$	$\Lambda_c\bar{D}$	$\Lambda_c\bar{D}^*$	Total
				1		N/A			0.08	1.08
$\frac{3}{2}^-$	$C[111]F[21]S[21][\chi_1]$			0.88		0.03			0.10	1.01
				0.86		0.03			0.10	0.99
						N/A				N/A
	$C[21]F[21]S[3][\chi_1]$					0.34				0.34
						0.34				0.34
						N/A				N/A
	$C[21]F[21]S[3][\chi_0]$					0.20				0.20
						0.21				0.21
						N/A			0.31	0.31
	$C[21]F[21]S[21][\chi_1]$					0.13			0.40	0.53
						0.14			0.39	0.53

Continued on next page

Table 3.7 The partial width ratio results of P_c configuration with I = $\frac{1}{2}$ for $P_c(4312)$, $P_c(4440)$ and $P_c(4457)$ which are normalized by $P_c(4312) \to pJ/\psi$ as reference channel (Continued).

J^p	P_c configuration	$\Delta J/\psi$	$\Delta\eta_c$	pJ/ψ	$p\eta_c$	$\Sigma_c^*\bar{D}$	$\Sigma_c\bar{D}$	$\Lambda_c\bar{D}$	$\Lambda_c\bar{D}^*$	Total
				1			N/A	0.07	0.02	1.09
$\frac{1}{2}^-$	$C[111]F[21]S[21][\chi_1]$			0.88			0.01	0.06	0.03	0.97
				0.86			0.01	0.06	0.03	0.96
					0.90		N/A	0.02	0.06	0.98
	$C[111]F[21]S[21][\chi_0]$				0.79		0.03	0.02	0.08	0.92
					0.77		0.03	0.02	0.07	0.89
							N/A			N/A
	$C[21]F[21]S[3][\chi_1]$						0.54			0.54
							0.53			0.53
							N/A	0.29	0.08	0.37
	$C[21]F[21]S[21][\chi_1]$						0.03	0.24	0.10	0.37
							0.03	0.24	0.10	0.37

Continued on next page

Table 3.7 The partial width ratio results of P_c configuration with I = $\frac{1}{2}$ for $P_c(4312)$, $P_c(4440)$ and $P_c(4457)$ which are normalized by $P_c(4312) \rightarrow pJ/\psi$ as reference channel (Continued).

J^p	P_c configuration	$\Delta J/\psi$	$\Delta\eta_c$	pJ/ψ	$p\eta_c$	$\Sigma_c^*\bar{D}$	$\Sigma_c\bar{D}$	$\Lambda_c\bar{D}$	$\Lambda_c\bar{D}^*$	Total
							N/A	0.10	0.23	0.33
	$C[21]F[21]S[21][\chi_0]$						0.10	0.08	0.30	0.48
							0.10	0.08	0.30	0.48

CHAPTER IV

DISCUSSIONS AND CONCLUSIONS

In this thesis, we studied the P_c states in the compact pentaquark picture. We constructed all possible wave functions by group theory. There are totally 17 states including the quantum number in terms of isospin and total spin (I, J^P) as $(\frac{3}{2}, \frac{5}{2}^-)$, $(\frac{3}{2}, \frac{3}{2}^-)$, $(\frac{3}{2}, \frac{1}{2}^-)$, $(\frac{1}{2}, \frac{5}{2}^-)$, $(\frac{1}{2}, \frac{3}{2}^-)$, and $(\frac{1}{2}, \frac{1}{2}^-)$.

By energy conservation, the possible decay channels are $p\eta_c$, $\Delta\eta_c$, pJ/ψ, $\Delta J/\psi$, $\Lambda_c\bar{D}$, $\Sigma_c\bar{D}$, $\Sigma_c^*\bar{D}$ and $\Lambda_c\bar{D}^*$. Among these 17 pentaquark configurations, the state $C[21]F[21]S[3][\chi_1]$ with total spin 5/2 has no allowed channel in all of the eight possible final states. Thus, we did not include this state in this study.

We studied the partial width ratios of each P_c configuration in Tables 3.4 and 3.5, which chooses one mode as a reference channel. The other modes in the same configuration are calculated corresponding to this reference channel. The three P_c in the experimental observations are described in any of these 17 configuration states because the experimental reports have not determine the isospin and spin of each P_c state. The spins of $P_c(4312)$, $P_c(4440)$ and $P_c(4457)$ are suggested by LHCb as $\frac{1}{2}$, $\frac{1}{2}$, and $\frac{3}{2}$, respectively. The results of Tables 3.4 and 3.5 show that the pJ/ψ channel is open for only two states in the isospin 1/2 configuration which are $C[111]F[21]S[21][\chi_1]$ with spin $\frac{3}{2}$ and $\frac{1}{2}$. For the configuration $C[111]F[21]S[21][\chi_1]$ with spin $\frac{3}{2}$, the $P_c(4312)$ has one more open charm decay channel ($\Lambda_c\bar{D}^*$) while $P_c(4440)$ and $P_c(4457)$ have two more open charm decay channels ($\Sigma_c^*\bar{D}$ and $\Lambda_c\bar{D}^*$). For the configuration $C[111]F[21]S[21][\chi_1]$ with spin $\frac{1}{2}$, $P_c(4312)$ has two more open charm decay channels ($\Lambda_c\bar{D}$ and $\Lambda_c\bar{D}^*$) while $P_c(4440)$ and $P_c(4457)$ have three more open charm decay channels ($\Sigma_c\bar{D}$, $\Lambda_c\bar{D}$ and $\Lambda_c\bar{D}^*$). In addition, the pJ/ψ channel is still dominant over the open charm decay channels in each P_c configuration.

In another consideration, the four $I = \frac{1}{2}$ and $J = \frac{3}{2}$ states in Table 3.6 could linearly combine to form four physical states. The same goes with the five $I = \frac{1}{2}$ and $J = \frac{1}{2}$ states in Table 3.7. Therefore, there could possibly be nine charmonium-like pentaquark states, which may decay into pJ/ψ. Based on the decay ratios in Tables 3.6 and 3.7, we suggest charmonium-like pentaquarks to be searched in other channels too, especially in the $p\eta_c$ channel. Experimental data of decay branching widths to all dominant channels are key to reveal the nature of these charmonium-like pentaquark states.

If there is no mixing among the $I = \frac{1}{2}$ and $J = \frac{3}{2}$ states as well as among the $I = \frac{1}{2}$ and $J = \frac{1}{2}$ states, there are only two states with the pentaquark configuration $C[111]F[21]S[21][\chi_1]$ that may decay through the pJ/ψ channel. Therefore, one may describe only two of the three observed P_c in the compact pentaquark picture. Meanwhile, we employed the $P_c(4312) \to pJ/\psi$ channel to normalize the all allowed channels for $I = \frac{1}{2}$ which are shown in Table 3.7. Our results show that the configuration $C[111]F[21]S[21][\chi_1]$ states with spin $\frac{3}{2}$ and $\frac{1}{2}$ have the same decay width ratios in the pJ/ψ decay channel which indicates that $P_c(4440)$ may not be a compact pentaquark since its decay width is much larger than the other observed P_c. This results suggest that one may assign $J = \frac{1}{2}$ to $P_c(4312)$ and $J = \frac{3}{2}$ to $P_c(4457)$.

In the future, if the experimental branching ratios does appear in the decay channels $p\eta_c$, $\Lambda_c\bar{D}$ and $\Lambda_c\bar{D}^*$ larger than pJ/ψ, then $P_c(4312)$ may not be a compact pentaquark. Also if the experimental branching ratio of $\Delta\eta_c$ is less than pJ/ψ, then $P_c(4312)$ may also not be a compact pentaquark because the our calculation of width ratios get the opposite way. Even though the partial width ratios of the four possible open charm decay channels are small when they normalized by $P_c(4312) \to pJ/\psi$, they may probably be found in a future experiment. So far we have only observed $P_c \to PJ/\psi$, the remaining seven possible decay channels should be searched in the future for pentaquark. However, the study of hidden charm pentaquarks needs more experimental information to confirm its structure. This thesis serves a model to learn about the structure of P_c in the compact pentaquark picture.

REFERENCES

REFERENCES

Aaij, R., Adeva, B., Adinolfi, M., Affolder, A., Ajaltouni, Z., Akar, S., Albrecht, J., Alessio, F., Alexander, M., Ali, S., Alkhazov, G., Cartelle, P. A., Jr, A. A., Amato, S., Amerio, S., et al. (2015). Observation of $J/\psi p$ Resonances Consistent with Pentaquark States in $\Lambda_b^0 \to J/\psi K^- p$ Decays. **Phys. Rev. Lett.** 115: 072001.

Aaij, R., Abellán Beteta, C., Ackernley, T., Adeva, B., Adinolfi, M., Afsharnia, H., Aidala, C., Aiola, S., Ajaltouni, Z., Akar, S., and al., et (2020). First observation of the decay Λb0→ηc(1S)pK−. **Physical Review D** 102(11).

Aaij, R., Beteta, C. A., Adeva, B., Adinolfi, M., Aidala, C. A., Ajaltouni, Z., Akar, S., Albicocco, P., Albrecht, J., Alessio, F., Alexander, M., Albero, A. A., Alkhazov, G., Cartelle, P. A., Jr, A. A. A., et al. (2019). Observation of a narrow pentaquark state, $P_c(4312)^+$, and of two-peak structure of the $P_c(4450)^+$. **Phys. Rev. Lett.** 122(22): 222001.

Abazov, V. M., Abbott, B. K., Acharya, B. S., Adams, M. R., Adams, T., Agnew, J. P., Alexeev, G. D., Alkhazov, G. D., Alton, A. K., Askew, A. W., Atkins, S., Augsten, K., Aushev, V., Aushev, Y., Avila, C. A., et al. (2019). Inclusive production of the P_c resonances in $p\bar{p}$ collisions. (arXiv:1910.11767).

ATLAS (2019). Study of $J/\psi p$ resonances in the ${}^0_b{\to}J/\psi p K^-$ decays in pp collisions at $\sqrt{s}$=7 and 8TeV with the ATLAS detector. (ATLAS-CONF-2019-048).

Barnes, V. E., Connolly, P. L., Crennell, D. J., Culwick, B. B., Delaney, W. C., Fowler, W. B., Hagerty, P. E., Hart, E. L., Horwitz, N., Hough, P. V. C., Jensen, J. E., Kopp, J. K., Lai, K. W., Leitner, J., Lloyd, J. L., et al. (1964). Observation of a Hyperon with Strangeness Minus Three. **Phys. Rev. Lett.** 12 (8): 204–206.

Gell-Mann, M. (1964). A Schematic Model of Baryons and Mesons. **Phys. Lett.** 8: 214–215.

Gutsche, T., Faessler, A., Yen, G. D., and Yang, S. N. (1997). Consequences of strangeness content in the nucleon for φ - meson production in $N\bar{N}$ annihilation. **Nuclear Physics B - Proceedings Supplements** 56(1): 311 –316.

Gutsche, T., Vinh Mau, R., Strohmeier-Presicek, M., and Faessler, A. (1999). Radiative proton-antiproton annihilation and isospin mixing in protonium. **Phys. Rev. C** 59 (2): 630–641.

Le Yaouanc, A., Oliver, L., Pene, O., and Raynal, J. (1988). *HADRON TRANSITIONS IN THE QUARK MODEL*.

Limphirat, A., Kobdaj, C., Suebka, P., and Yan, Y. (2010). Decay widths of ground-state and excited Ξ_b baryons in a nonrelativistic quark model. **Phys. Rev. C** 82 (5): 055201.

Liu, Y.-R., Chen, H.-X., Chen, W., Liu, X., and Zhu, S.-L. (2019). Pentaquark and Tetraquark states. **Prog. Part. Nucl. Phys.** 107: 237–320.

Srisuphaphon, S., Kaewsnod, A., Limphirat, A., Khosonthongkee, K., and Yan, Y. (2016). Role of pentaquark components inϕmeson production proton-antiproton annihilation reactions. **Physical Review C** 93(2).

Vandermeulen, J. (1988). $N\bar{N}$ Annihilation creates two mesons. 37 (4).

Yan, Y, Khosonthongkee, K, Kobdaj, C, and Suebka, P (2010). $e^+e^- \to \bar{N}N$ at threshold and proton form factor. **Journal of Physics G: Nuclear and Particle Physics** 37(7): 075007.

Yan, Y., Kobdaj, C, Uchai, W, Faessler, A., Gutsche, T, and M. Zheng, Y (Feb. 2003). e+e- annihilation into NN pairs. **Modern Physics Letters A** 18: 370–373.

Yao, W. M., Amsler, C., Asner, D., Barnett, R. M., Beringer, J., Burchat, P. R., Carone, C. D., Caso, C., Dahl, O., D'Ambrosio, G., DeGouvea, A., Doser, M., Eidelman, S., Feng, J. L., et al. (2006). Review of Particle Physics, 2006-2007. Review of Particle Properties. **J. Phys. G** 33: 1–1232.

Zweig, G. (1964). An SU(3) model for strong interaction symmetry and its breaking. Version 1.

APPENDICES

APPENDIX A

PERMUTATION GROUP

In this thesis, we consider the baryon which corresponds to S_3 permutation group. This permutation has 3! or 6 members : e, (12), (13), (23), (123),(132).
The conjugacy class of S_3 can be represented by Young tabloids. Young tabloids can be systemically constructed by the following rules:
(1) Number of the box equal to number of n in S_n
(2) Number of the top box and right box always larger than or equal to the below and left box

For the 3-quarks, we employed S_3 permutation group. The Young tabloids have 3 irreducible representation which are [3], [21], and [111].

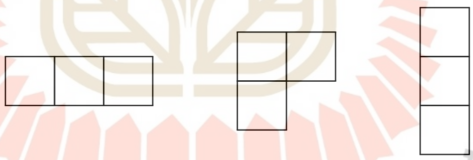

We can label and fill the number of each box to determine the dimensions of irreducible representation. Young tableaux can be constructed by the following rules:
(1) the number in a box differs from any number in other boxes.
(2) the numbers in a row must increase from left to right.
(3) the numbers in a column must increase from top to bottom.

Therefore, the dimension can correspond to Young tableaux and be listed below:

$$[3]: \quad \begin{array}{|c|c|c|}\hline 1 & 2 & 3 \\ \hline \end{array} \qquad r = 1$$

$$[21]: \quad \begin{array}{|c|c|}\hline 1 & 2 \\ \hline 3 & \multicolumn{1}{c}{} \\ \cline{1-1} \end{array} \quad \begin{array}{|c|c|}\hline 1 & 3 \\ \hline 2 & \multicolumn{1}{c}{} \\ \cline{1-1} \end{array} \qquad r = 2$$

$$[111]: \quad \begin{array}{|c|}\hline 1 \\ \hline 2 \\ \hline 3 \\ \hline \end{array} \qquad r = 1$$

where r is dimension of irreducible representation.

We know the singlet representation in the Young tabloids is [111] in case of 3-quarks when we put the different quarks (u, d, and s) or color (R, G, and B) into the boxes. We must get only one possible which follow the dimension. In case of the P_c, we also get the singlet as [222].

The group elements of permutation group can be defined by Yamanouchi basis. The Yamanouchi basis utilized in this thesis is written in the form

$$\phi^{[\lambda]}_{(r)} = |[\lambda(r_n, r_{n-1}, ..., r_2, r_1)]\rangle \tag{A.1}$$

where $[\lambda]$ is the young tabloid, r_i stands for the row from which a box is removed in the order of large number to small number.

The operation of the element (n − 1, n) on the standard basis of S_n follows the rules:

$$\begin{aligned} (n{-}1, n)\, |[\lambda](r, r, r_{n-2}, ..., r_2, 1)\rangle &= +\, |[\lambda](r, r, r_{n-2}, ..., r_2, 1)\rangle \\ (n{-}1, n)\, |[\lambda](r, r{-}1, r_{n-2}, ..., r_2, 1)\rangle &= -\, |[\lambda](r, r{-}1, r_{n-2}, ..., r_2, 1)\rangle \end{aligned} \tag{A.2}$$

when $|[\lambda](r{-}1, r, r_{n-2}, ..., r_2, 1)\rangle$ not exists, and

$$(n{-}1, n)\,|[\lambda](r, s, r_{n-2}, ..., r_2, r_1)\rangle = \sqrt{1-\sigma_{rs}^2}\,|[\lambda](s, r, r_{n-2}, ..., r_2, r_1)\rangle \\ +\sigma_{rs}\,|[\lambda](r, s, r_{n-2}, ..., r_2, r_1)\rangle \tag{A.3}$$

when $|[\lambda](r, s, r_{n-2}, ..., r_2, r_1)\rangle$ and $|[\lambda](s, r, r_{n-2}, ..., r_2, r_1)\rangle$ all exist and r $\neq$ s. For $[\lambda] = [\lambda_1, \lambda_2, ..., \lambda_r ... \lambda_s ... \lambda_n]$, we have

$$\sigma_{rs} = \frac{1}{(\lambda_r{-}r){-}(\lambda_s{-}s)} \tag{A.4}$$

For other elements there is an additional formula from group theory,

$$(i, n) = (n{-}1, n)(i, n{-}1)(n{-}1, n) \tag{A.5}$$

.

Finally, we get the group element for S_3 which are shown below:

(1) Matrix representation of $S_3[3]$

$$D^{[3]}(12) = D^{[3]}(13) = D^{[3]}(23) = \begin{pmatrix} 1 \end{pmatrix}$$

2) Matrix representation of $S_3[21]$

$$D^{[21]}(12) = \begin{pmatrix} 1 & 0 \\ 0 & -1 \end{pmatrix} \qquad D^{[21]}(13) = \begin{pmatrix} -1/2 & -\sqrt{3}/2 \\ -\sqrt{3}/2 & 1/2 \end{pmatrix}$$

$$D^{[21]}(23) = \begin{pmatrix} -1/2 & \sqrt{3}/2 \\ \sqrt{3}/2 & 1/2 \end{pmatrix}$$

(3) Matrix representation of $S_3[111]$

$$D^{[3]}(12) = D^{[3]}(13) = D^{[3]}(23) = \begin{pmatrix} -1 \end{pmatrix}$$

APPENDIX B

PROJECTION OPERATORS

The explicit form of the baryon spin and flavor functions can be easily derived in the framework of the Yamanouchi basis developed in the permutation group. One needs to work out the projection operators for the Young tableaux of the multiplet states, and then act the operators onto certain state configurations. The projection operators corresponding to the Yamanouchi basis function $|[\lambda](r)\rangle_i$ of the representation $[\lambda]$ of S_n take the form

$$W_{(r)}^{[\lambda]} = \sum_i \langle[\lambda](r)|\, P_i \,|[\lambda](r)\rangle\, P_i \tag{B.1}$$

where P_i stand for all the permutations of S_n.

We directly worked out the projection operators of S_3, which are written by

$$\begin{aligned}
P^S &= 1 + (12) + (13) + (23) + (123) + (132) \\
P^\lambda &= 1 + \frac{1}{2}(12) - \frac{1}{2}(13) - \frac{1}{2}(23) - \frac{1}{2}(123) - \frac{1}{2}(132) \\
P^\rho &= 1 - \frac{1}{2}(12) + \frac{1}{2}(13) + \frac{1}{2}(23) - \frac{1}{2}(123) - \frac{1}{2}(132) \\
P^A &= 1 - (12) - (13) - (23) + (123) + (132)
\end{aligned} \tag{B.2}$$

where P^S, P^ρ, P^ρ, and P^A are the projection operators for symmetric, λ-type symmetric, ρ-type symmetric, and antisymmetric state, respectively. For example, we applied the projection on the flavor state uud (with u $\equiv \phi_u$ and d $\equiv \phi_d$) as

For flavor symmetric wave function([3]),

- $\begin{array}{|c|c|c|}\hline 1 & 2 & 3 \\ \hline \end{array}, \begin{array}{|c|c|c|}\hline u & u & d \\ \hline \end{array}$

$$\begin{aligned} P^S u_1u_2d_3 &= u_1u_2d_3 + u_2u_1d_3 + d_3u_2u_1 + u_1d_3u_2 + u_2d_3u_1 + d_3u_1u_2 \\ &= 2uud + 2udu + 2duu \\ \Rightarrow \phi^S &= \frac{1}{\sqrt{3}}(uud + duu + udu) \end{aligned} \tag{B.3}$$

For flavor mixed-type wave function ([21]),

- $\begin{array}{|c|c|}\hline 1 & 2 \\ \hline 3 & \multicolumn{1}{c}{} \\ \cline{1-1} \end{array}, \begin{array}{|c|c|}\hline u & u \\ \hline d & \multicolumn{1}{c}{} \\ \cline{1-1} \end{array}$

$$\begin{aligned} P^\lambda u_1u_2d_3 &= u_1u_2d_3 + u_2u_1d_3 - \frac{1}{2}d_3u_2u_1 - \frac{1}{2}u_1d_3u_2 - \frac{1}{2}u_2d_3u_1 - \frac{1}{2}d_3u_1u_2 \\ &= 2uud - udu - duu \\ \Rightarrow \phi^\lambda &= \frac{1}{\sqrt{6}}(2uud - duu - udu) \end{aligned} \tag{B.4}$$

- $\begin{array}{|c|c|}\hline 1 & 3 \\ \hline 2 & \multicolumn{1}{c}{} \\ \cline{1-1} \end{array}, \begin{array}{|c|c|}\hline u & u \\ \hline d & \multicolumn{1}{c}{} \\ \cline{1-1} \end{array}$

$$\begin{aligned} P^\rho u_1d_2u_3 &= u_1d_2u_3 - d_2u_1u_3 + \frac{1}{2}u_3d_2u_1 + \frac{1}{2}u_1u_3d_2 - \frac{1}{2}d_2u_3u_1 - \frac{1}{2}u_3u_1d_2 \\ &= \frac{3}{2}udu - \frac{3}{2}duu \\ \Rightarrow \phi^\rho &= \frac{1}{\sqrt{2}}(udu - duu) \end{aligned} \tag{B.5}$$

APPENDIX C

WIGNER'S 9-J SYMBOLS

In the calculation of pentaquark system, the changing of states with coupled pair of quarks for final state were necessary to prepare state for easier calculation. Wigner's 9j symbols mainly employed in the coupling of four angular momenta. Suppose that there are four angular momenta $\vec{J}_1$, $\vec{J}_2$, $\vec{J}_3$ and $\vec{J}_4$, the simultaneous eigenstates of the operators $|J_i^2, J_{iz}\rangle$ are $|j_i m_i\rangle$. The direct product states

$$|j_1 j_2 j_3 j_4; m_1 m_2 m_3 m_4\rangle \equiv |j_1 m_1\rangle\,|j_2 m_2\rangle\,|j_3 m_3\rangle\,|j_4 m_4\rangle \tag{C.1}$$

are the eigenstates of the operators $|J_i^2, J_{iz}\rangle$. For given j_i with i = 1, 2, 3, 4, these states form a complete basis in the direct product space of dimension $(2j_1+1)(2j_2+1)(2j_3+1)(2j_4+1)$ with transformation corresponding to the direct product representation

$$D(\vec{\lambda}) = D^{j_1}(\vec{\lambda}) \otimes D^{j_2}(\vec{\lambda}) \otimes D^{j_3}(\vec{\lambda}) \otimes D^{j_4}(\vec{\lambda}) \tag{C.2}$$

we get the infinitesimal operator is $J = J_1 + J_2 + J_3 + J_4$. There are different ways to couple the four angular momenta to get the same total angular momentum, For example

$$|(j_1 \otimes j_2)_{j_{12}} \otimes (j_3 \otimes j_4)_{j_{34}}; jm\rangle \tag{C.3}$$

or

$$|(j_1 \otimes j_3)_{j_{13}} \otimes (j_2 \otimes j_4)_{j_{24}}; jm\rangle \tag{C.4}$$

The relation between the above bases is

$$|(j_1 \otimes j_2)_{j_{12}} \otimes (j_3 \otimes j_4)_{j_{34}}; jm\rangle = \sum_{j_{13}j_{24}} \langle (j_1 j_3)_{j_{13}} (j_2 j_4)_{j_{24}}; jm | (j_1 j_2)_{j_{12}} (j_3 j_4)_{j_{34}}; jm\rangle$$
$$|(j_1 \otimes j_3)_{j_{13}} \otimes (j_2 \otimes j_4)_{j_{24}}; jm\rangle \tag{C.5}$$

with

$$\langle (j_1 j_3)_{j_{13}} (j_2 j_4)_{j_{24}}; jm | (j_1 j_2)_{j_{12}} (j_3 j_4)_{j_{34}}; jm\rangle$$
$$\sqrt{(2j_1+1)(2j_2+1)(2j_3+1)(2j_4+1)} \begin{Bmatrix} j_1 & j_2 & j_{12} \\ j_3 & j_4 & j_{34} \\ j_{13} & j_{24} & j \end{Bmatrix} \tag{C.6}$$

where

$$\begin{Bmatrix} j_1 & j_2 & j_{12} \\ j_3 & j_4 & j_{34} \\ j_{13} & j_{24} & j \end{Bmatrix}$$

is called Wigner's 9j symbols.

CURRICULUM VITAE

NAME: Wiriya Ruangyoo **GENDER**: Male

NATIONALITY: Thai **DATE OF BIRTH**: June 20, 1995

E-MAIL: wiriya_bright@hotmail.com

EDUCATIONS:

- 2007 - 2013, High school at Uttaradit school
- 2013 - 2017, Bachelor of Science, Department of Physics , Institute of Science, Naresuan University
- 2017 - 2020, Master of Science, School of Physics, Institute of Science, Suranaree University of Technology
- 2019 - 2020, Double/Dual master degree program between Department of Physics, National Cheng Kung University, Taiwan and School of Physics, Institute of Science, Suranaree University of Technology.

EXPERIENCE:

- Co-operative education in Physics nuclear and particle group, School of physics, Institute of Science, Suranaree University of Technology on 9 January-28 May 2017
- Participated in the Machine and Deep Learning Workshop at Suranaree University

SCHOLARSHIPS:

- Royal Thai Scholarship from the Development and Promotion of Science and Technology Talents Project (DPST)